# EFFECTS OF DOPANTS ON THE CONDUCTIVITY OF POLYANILINE SYNTHESIZED BY CHEMICAL OXIDATION AND ELECTROCHEMICAL METHODS



By

**AWUAH, Joseph Asare**

**(BSc Physics – Materials Science)**

**A Thesis submitted to the Department of Physics, Kwame Nkrumah University of Science and Technology, in partial fulfillment of the requirement for the degree of**

**MASTER OF PHILOSOPHY (MATERIALS SCIENCE)**

**College of Science**

**AUGUST, 2019**

## DECLARATION

I hereby declare that this submission is my own work towards the MPhil and that, to the best of my knowledge, it contains no material previously published by any person nor material which has been accepted for the award of any other degree of the University, except where due acknowledgement has been made in the text.



AWUAH, Joseph Asare (20484969)

……. …… ……..

Student Signature Date

Certified by:

**Prof. K. Singh**

…… …… ….…….

Supervisor Signature Date

Certified by:

**Mr. O. A. Nunoo**

…… …… …….

Supervisor Signature Date

Certified by:

**Prof. R.Y. Tamakloe** …… ……..……..

Head of Department Signature Date

## DEDICATION

I dedicate this work to my entire family.



## ACKNOWLEDGEMENT

My deepest gratitude goes out to my Supervisors Prof. K. Singh and Mr. O. A. Nunoo. I also thank Dr. E. K. Abavare and Mr. Isaac Nkrumah of the Physics Department, KNUST for their advice and support. I would also like to thank Mr. Paal Mark and Mr. Amoah of the Physics Department for their assistance during the preparation of samples. To all my colleagues at the Department of Physics I say a very big thank you.



## ABSTRACT

Polyaniline salts (PANI-ES) were synthesized by chemical and electrochemical oxidation using primary dopants such as HCL, $HNO_3$, $H_2SO_4$ and $CH_3COOH$ and the aniline as the monomer. All the synthesized PANI have resulted in emeraldine salts form as indicated by dark green colour of the salts. Various characterization techniques employed were UV-Visible spectroscopy, FT-IR and Cyclic voltammetery studies. All these techniques confirm the various properties of PANI. The characteristic bands in UV-Visible spectra of the samples indicate that effective doping has occurred in the synthesized polymer. Quinoid and benzenoid peaks at 1553-1596 $cm^{-1}$ and 1437 – 1496 $cm^{-1}$ respectively were observed in all the samples. The band gaps for all the samples, both bulk and thin film, were obtained using the absorption spectra and Stern relation. PANI-$H_2SO_4$ had the least band gap for both bulk and thin film samples whereas PANI-$CH_3COOH$ had the highest band gap. The voltammogram showed the various oxidation states during the electrochemical deposition at potential of 0.8 V. Four probe method was used to study the conductivity of both thin and bulk samples. The conductivity values for PANI-$H_2SO_4$ were found to be highest i.e. 1.183 $S.cm^{-1}$ and 3.424 $S.cm^{-1}$ for bulk and thin film respectively.

## TABLE OF CONTENTS

**Declaration……i**

**Dedication ……ii**

**Acknowledgement……...iii**

**Abstract…….……....iv**

**Table of Content…….....v-vi**

**List of Tables……...vii**

**List of Tables…..……..viii**

**1.1 INTRODUCTION..... iv**

**Structure of PANI .....2**

**OBJECTIVES OF THE PROJECT WORK ..... 5**

**2.2 THEORY OF ELECTRICAL CONDUCTION IN CONDUCTING POLYMERS ..... 11**

**2.3 EXPERIMENTAL TECHNIQUES ..... 16**

**2.3.1 Synthesis of polyaniline (PANI)..... 16**

**2.3.2 Chemical Oxidative Synthesis.....17**

**2.3.4 Electrochemical Oxidative iSynthesis .....18**

**2.4 Characterization Techniques..... 21**

**2.4.1 UV-Vis-NIR Spectroscopy .....21**

**2.4.2 FTIR Spectroscopy.....24**

**2.4.3 Cyclic Voltammetry.....26**

**2.3.4 Thin iFilm Thickness iMeasurements iTechniques .....28**

**2.4.5 Electrical Conductivity iMeasurements .....30**

**4-Point Probe .....32**

**3.1 Synthesis of Polyaniline (PANI)..... 34**

**3.1.1 Polymerization Process (Chemical Oxidation) .....34**

**3.1.2 Electrochemical Oxidation Using Different Dopants.....35**

**3.2 CHARACTERISATION OF SAMPLES ..... 35**
**3.2.1 FOURIE TRANSFORM INFRARED SPECTROSCOPY (FTIR) .....35**
**3.2.2 ULTRAVIOLET-VISIBLE SPECTROCOPY (UV-Vis) .....36**
**3.2.3 CYCLIC VOLTAMMETRY.....36**
**3.2.4 CONDUCTIVITY .....37**
**4.1 FOURIER TRANSFORMATION INFRARED SPECTROSCOPY (FTIR) ..... 38**
**4.2 UV-Vis OF BULK SAMPLES ..... 48**
**4.2.1 Determination of the Band Gap of Bulk Samples.....50**
**4.3 UV-Vis OF THIN FILM SAMPLES..... 51**
**4.3.1 Determination the Band Gap of Thin Film Samples .....52**
**4.CYCLIC VOLTAMMOGRAMS OF THIN FILMS ..... 54**
**4.5 CONDUCTIVITY OF SAMPLES ..... 56**
**CONCLUSION AND RECOMMENDATION.....61**
**5.1 CONCLUSION .....61**
**5.2 RECOMMENDATION .....62**
**APPENDICES**.....66-70

**LIST OF TABLES**

Table 4.0: Identified Bonds from FTIR of Thin films ……45

Table 4.1: Identified Bonds from FTIR of Bulk Samples ……...…50

Table 4.2: Band gap values for Thin films and Bulk Samples ……...…59

Table 4.3: Data for determination of thickness of Thin films……..63

Table 4.4: Data for determination of thickness of Bulk Samples ……...63

Table 4.5: Resistivity and Conductivity of Thin films ……63

Table 4.6: Resistivity and Conductivity of Bulk Samples……...63

**LIST OF FIGURES**

Figure 1.1: Aniline monomer…….2

Figure 1.2: Generalised structure of Polyaniline ……..3

Figure 1.3: Different forms of PANI…….4

Figure 2.1: Molecular orbitals in a diatomic molecule……..…12

Figure 2.2: Different forms of PANI with Polarons and Bipolarons……15

Figure 2.3: Electrodeposition by Potentiostatic Method ……...….20

Figure 2.4: Cyclic Voltammogram of PANI……..…..27

Figure 2.5: Circuit diagram for Two-point probe on a Sample……32

Figure 2.6: Circuit diagram for Four-point probe on a Sample ……..…..…32

Figure 4.1: FTIR of PANI-$CH_3COOH$ Thin film…….……39

Figure 4.2: FTIR of PANI-$HNO_3$ Thin film ……...……...40

Figure 4.3: FTIR of PANI-$H_2SO_4$ Thin film ……..…41

Figure 4.4: FTIR of PANI-HCl Thin film…….……42

Figure 4.5: FTIR of PANI-$HNO_3$ Bulk Sample……43

Figure 4.6: FTIR of PANI- $H_2SO_4$ Bulk Sample…….44

Figure 4.7: FTIR of PANI-HCl Bulk Sample……..45

Figure 4.8: FTIR of PANI- $CH_3COOH$ Bulk Sample…….....……46

Figure 4.9: Absorbance versus Wavelength of Bulk Samples…….47

Figure 4.10: Band Gap of Bulk Samples……..50

Figure 4.11: Absorbance versus Wavelength of Thin Films……51

Figure 4.12: Band Gap of Thin films……52

Figure 4.13: Cyclic Voltamographs of Thin films……...….53

Figure 4.14: Conductivity versus Type of Dopant……....57

# CHAPTER ONE

## INTRODUCTION

Polymers are a class of materials that are important to our everyday life. Cabinets, plastic cutlery and latex paints are examples of polymers that are used every day. They are giant molecules of high molecular weight which are built up by linking together large numbers of smaller molecules called monomers. The reaction by which the monomers combine to form a huge polymer is known as polymerization (Gowariker et al., 1986). Traditionally polymers were thought of as insulators when it comes to its applications in electronics. In the mid-19th century scientist conducted research into some organic based polymers for their application in electronics (Inzelt, 2008). In the case of polypyrrole it was observed that it had resistivity as low as 1 ohm/cm (Bolto et al., 1963). (Songxi, 2012) cites multiple reports of similar high conductivity oxidized polyacetylenes. DeSurville and coworkers reported high conductivity in polyaniline (De Surville et al., 1968). In 1980, Diaz and Logan also reported films of polyaniline that can serve as electrodes (Diaz et al., 1980). Hideki Shirikawa, Alan MacDiarmid and Alan J. Heeger in 1977 published a paper on the high conductivity in oxidized iondine-doped polyacetylene (Shirikawa et al., 1977). They were awarded the 2000 Nobel Prize in Chemistry for the discovery and development of conductive polymers (Natarajah, 2012).

Lightfoot's studies on the oxidation of aniline in 1860s led to the discovery of polyaniline (MacDiarmid, 2001). The first definitive report of polyaniline did not occur until 1862, which included an electrochemical method for the determination of small quantities of aniline (Letheby, 1862). Only since the early 1980s has polyaniline captured the intense attention of the scientific community. This interest is due to the rediscovery of high electrical conductivity. Amongst the family of conducting polymers and organic semiconductors, polyaniline has many attractive

processing properties (Pandya, 2016). Polyaniline (PANI) is one of the most studied conjugated polymers due to its widely tunable electrical conductivity (Cao et al., 1992) and environmental stability (Rannou and Nechtschein, 1997, DeLongchamp and Hammond, 2001). PANI can be readily synthesized from commercially available starting materials under mild conditions by oxidation methods (Masters et al., 1991), (Wei et al., 1989). Polyaniline remains one of the most interesting materials due to its unique conduction mechanism and good environmental stability in the presence of oxygen and water (Kumar et. al.,1997).

**Structure of PANI**

Polyaniline is obtained from the monomer aniline. Aniline is an organic compound with the formula $C_6 H_5 NH_2$. Consisting of a phenyl group attached to an amino group, aniline is the prototypical aromatic amine. Its main use is in the manufacture of precursors to polyurethane and other industrial chemicals. Like most volatile amines, it has the odor of rotten fish. It ignites readily, burning with a smoky flame characteristic of aromatic compounds (Kahl et al., 2000). Aniline is a planar molecule. The amine is nearly planar owing to conjugation of the lone pair with the aryl substituent.

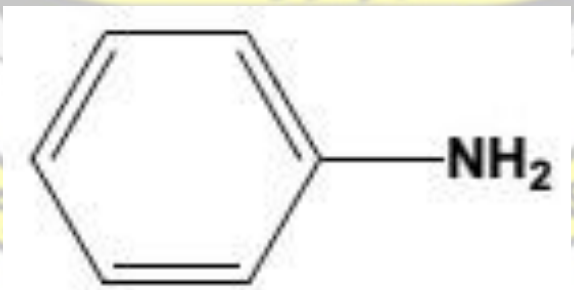


Figure 1.1: Aniline Monomer

The C-N distance is correspondingly shorter. In aniline, the C-N and C-C distances are close to 1.39 Å, indicating the $\pi$-bonding between N and C. Polyaniline has a rather unique polymeric structure which is mainly composed of sequentially alternating benzene rings and nitrogen atoms (Skotheim, 1997). The existence of nitrogen atoms as imine (in sp2 hybridized state) or amine (in sp3 hybridized state) forms, and their relative proportion in the overall polymer backbone chain determines the resulting structure and the different properties of polyaniline.

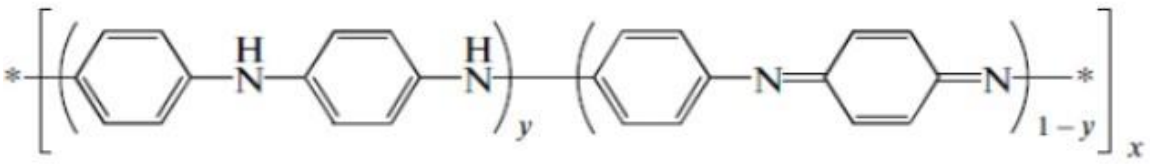

Figure 1.2: Generalised Structure of Polyaniline.

Polyaniline consists of monomer units built from reduced (y) and oxidized (1-y) blocks: where $0 \leq y \leq 1$. The redox state of the polymer is determined by the value of y, which may vary continuously from zero to unity. At y = 0.5, polyaniline occurs in the form of emeraldine, y = 0 corresponds to the fully oxidized form, permigraniline, while y = 1 corresponds to the fully reduced form, leucoemeraldine. Permigraniline and emeraldine may occur as either salts or bases. PANI has different forms with different colors, stabilities, and conductivities. Leucoemeraldine is a pale brown substance characterized by an absorption band at 343 nm (in Nmethylpyrrolidone) (Masters et al., 1991). The conducting form of polyaniline is emeraldine-salt (ES). The emeraldine base (EB) can be converted to ES by protonic acid doping or oxidative doping with aqueous acid. This

process is reversible and that makes polyaniline unique among the class of conducting polymers.

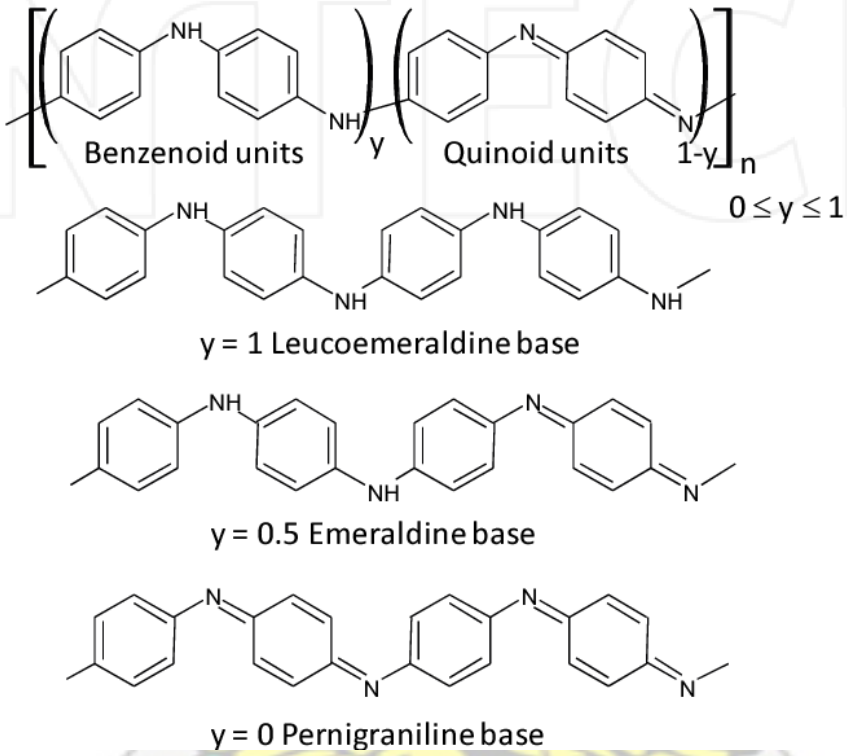


Figure 1.3: The Different forms of PANI

## OBJECTIVES OF THE PROJECT WORK

The main objectives of this thesis are to synthesize and study the properties of polyaniline (PANI). In this direction the following specific objectives have been achieved:

1. Synthesize (PANI) using four different dopants Hydrochloric acid (HCl) Sulfuric acid ($H_2SO_4$ ), Nitric acid ($HNO_3$ ) and Acetic acid ($CH_3COOH$) by chemical oxidative method.
2. Prepare thin films of polyaniline (PANI) by electrochemical oxidation polymerization technique.
3. Characterize the samples prepared using FTIR spectra to determine the functional groups and the dominant spectral peaks peculiar to PANI
4. Use UV-Vis spectrophotometer to determine some absorption peaks and also to determine $E_g$ values
5. To use cyclic voltammetry to observe the various oxidation states during the deposition of PANI onto ITO glass.
6. Measure the conductivity of the synthesized conducting polymer.

## REASONS FOR STUDYING THE EFFECT OF DOPANT ON THE PROPERTIES OF POLYANILINE

The processability, conductivity and stability are major requirements of any polymer for technological application (Chauhan *et al.,* 2010). Modifications of the oxidation state, dopant and polymerization conditions are means of optimizing the processability, conductivity and stability of

PANI for technological application. Researchers are interested in improving properties such as the electrical conductivity of PANI through the choice of appropriate dopants (Alesary et al., 2018). The ease of processability and electrical characteristics of polyaniline is why it has gained much attention among the other class of conducting polymers. Dopants create charge carriers in a conducting polymer which is responsible for the conductivity of the conducting polymer (Atassi et al., 2008). A study on the effects of primary dopants on the properties of Polyaniline will help in the determination of the most appropriate dopant for electrical and optical applications of the material.

**JUSTIFICATION OF THE PROJECT**

Although dopants have profound effect on the properties of PANI comparative study on the effects of dopant is relatively less (Sinha et al., 2008). The formation of charge carriers responsible for the conductivity of the materials is mostly achieved by the dopant. It is therefore essential to consider the type of dopant most appropriate in the synthesis of PANI and its influence in the conductivity of the material for technological applications. Some comparative study on the effect of different dopants (HCl and some organic acids) on the properties of PANI showed that the properties of doped PANI were function of the type of dopant (Sinha et al., 2009). To study the effect of primary acids as dopants on the properties of polyaniline will be an addition to the knowledge we have about the material.

## STRUCTURE OF THE THESIS

The thesis is in fix chapters: Chapter one gives an introduction to polymers and how there has been a shift from using polymers as insulators for electronic applications to them becoming essential in the semiconductor world. In this chapter also polyaniline is introduced and its uniqueness among the other class of conducting polymers is pointed out. The chapter also talks about the objectives for this work, reasons for interest in the effect of dopants on the properties of polyaniline and justification for the work is also given. The second chapter deals with the literature review, experimental techniques and relevant theory governing the work; conducting polymers, theory of conduction in conducting polymers, conduction mechanism in polyaniline and characterisation approaches to understanding the properties of polyaniline. The chapter three covers the methods and materials used in this project. The results in figures are represented and discussed in chapter four. Conclusion to the entire work and recommendations are presented in chapter five. There is an appendix at the end of the references.

# CHAPTER TWO

# LITERATURE REVIEW

## 2.1 CONDUCTING POLYMERS

Conductive polymers are organic polymers that conduct electricity (Inzelt, 2008). In general, conducting polymers include electronically conducting polymers and ionically conducting polymers. Ionically conducting polymers are usually called polymer electrolytes. Electronically conducting polymers can also include conjugated conducting polymers and the insulating polymers blending with conducting materials (Li et al., 2015). These compounds can be semiconductors. The advantage conductive polymers have is their processability. They can offer high electrical conductivity but do not show similar mechanical properties compared to other commercially available polymers. The electrical properties can be fine-tuned using the methods of organic synthesis (Naarmann, 2000) and by advanced dispersion techniques (Kasai et al., 2000). Most organic polymers were commonly regarded as electrical insulators by nature.

The first polymer with significant conductivity synthesized was polyacetylene from acetylene polyethene, as the monomer. Its electrical conductivity was discovered by Hideki Shirakawa, Alan Heeger, and Alan MacDiarmid who received the Nobel Prize in Chemistry in 2000 for this discovery. They synthesized this polymer for the first time in the year 1974 when they prepared polyacetylene as a silvery film from acetylene, using a Ziegler-Natta catalyst. Despite its metallic appearance, the first attempt did not yield a very conductive polymer. However, three years later, they discovered that oxidation with halogen vapor produces a much more conductive polyacetylene film Shirakawa et al. (1977). Conducting polymers are organic polymers that

conduct electricity. They can act as semiconductors or conductors. These polymers are conjugated.

Conjugated polymers are characterized by a backbone chain of alternating double and single bonds. Their overlapping p-orbitals create a system of delocalized $\pi$ -electrons, which can result in interesting and useful optical and electronic properties. The electrical conductivity of these polymers is based on the presence of conjugated double bonds along the polymer backbone. The strong chemical bonds between the carbon atoms are the so-called localized $\sigma$ bonds whereas the double bonds provide weaker and less strongly localized $\pi$ bonds. However, the inherent conductivity of these polymers is rather low. The structure of conducting polymers is usually composed of C, H and heteroatoms like Nitrogen (N) or oxygen (O) within a $\pi$ conjugated system (Hutchison et al., 2003).

Delocalized $\pi$ electrons originate from one unpaired electron per carbon atom in contrary to saturated polymers where all four valence electrons are used to constitute covalent chemical bonds. What all conducting polymers have in common is a high $\pi$ electron overlap along the polymer chain which facilitates the possibility of fast electron transfer. In spite of that fact, delocalization of $\pi$ electrons along the polymer backbone itself is not sufficient to obtain high conductivities and a process called doping is needed. Only when an electron is removed from the valence band by oxidation (p-doping) or added to the conducting band by reduction (n-doping) then the polymer become highly conductive. Through such a doping process, charge defects (polaron, bipolaron and soliton) are created that can travel through the backbone of the polymer.

Charge defects conceptually are not real particles, like electrons and holes, and that is why they are referred to as quasi-particles. Concerning their transport along the polymer backbone, the polarons and bi-polarons are distortions introduced into the structure of the polymer as a result of 'relaxation' occurring in the polymer as a result of the polymer system 'trying to adjust for the presence or introduction of an electric charge onto the polymer. Under applied electric field, these distortions, along with the associated charge (constituting a charged defect), are considered to propagate along the polymer backbone. Electronically, each charged defect has associated with it, an energy level in the energy gap and so conduction consists of transitions between these energy levels. As doping levels increase, more and more of these energy levels are formed in the energy gap, which eventually develop into a band, so that the conductivity of the doped polymer reaches metallic levels of conduction as transition between the energy levels within the band becomes almost continuous, like occurs in metals.

Solitons may be considered in the same light, conceptually, but they are exclusively formed in degenerate conducting polymers, like polyacetylene, and are formed as a neutral defect at a point in the polymer, where the order of the double-bond is reversed. It as a localized energy level associated with it (and so are its charged forms), right in the middle of the energy gap. Just as for the polarons and bipolarons, also form bands with increased doping, and that is why conductivity in polyacetylene is on record as having reached metallic levels of approximately, $10^5$ S/cm. So, the idea of these defects travelling in the conduction band is a little controversial. There are other models of conduction in doped conducting polymers, like the percolation theory and the Mott Variable Range Hopping. Unlike the case of traditional semiconductors where the doping levels

are very high, for example, about 1 dopant atom for every $10^{10}$ semiconductor atoms, in the case of organic conducting polymer doping, about 10% doping level can produce very appreciably high conductivity. For doped conducting polymers, the field of the counterions does not produce any net flow of current and so add nothing to the conduction in the polymer (Dissado et al., 1992).



Polythiophene (PT), polyaniline (PANI), poly (3,4-ethylenedioxythiophene) (PEDOT), poly(phenylene vinylene) (PPV), poly(p-phenylene vinylene) (PPV and polypyrrole (PPY) are conjugate polymers of great interest. This is because of their excellent chemical and electrochemical stability. They are easy to prepare in the form of large area thin films and can store charge throughout their entire volume. PPY and PANI can be formed chemically or electrochemically through oxidative polymerization of pyrrole and aniline monomers, the final form of PPY and PANI are those of a long-conjugated backbone.

## 2.2 THEORY OF ELECTRICAL CONDUCTION IN CONDUCTING POLYMERS

The electronic conducting property and conduction mechanism of conducting polymers (CPs) have been the major inspiration for studies by researchers with interest in the field (Poyraz, 2010). This significant property of CPs can be explained using the band gap model.

### 2.2.1 Band Theory as a Function of Application of molecular orbital Theory

The band theory originates from the formation of energy bands in materials from discrete energy levels found in single atom system. The chemical approach to band theory is to relate it to molecular orbital theory. In molecular orbital theory, using $H_1$ and $H_2$ hydrogen atoms as an

example (Fig 1.4), molecular orbital from $H_1$ atom can overlap with a molecular orbital of $H_2$ atom, resulting in the formation of two molecular orbitals known as the bonding (corresponding to the valence band) and antibonding (corresponding to the conduction) molecular orbitals (Peter Atkins, 2017). These are delocalized over both atoms, and the bonding molecular orbital possess lower energy than the $H_1$ and $H_2$ atomic orbital, while the antibonding molecular orbital has higher energy. The energy band that results from the bonding orbitals of a molecule is known as the valence band, while the conduction band is due to the antibonding orbitals of the molecule. The width of individual bands across the range of energy levels is called band width (Molapo *et al.*, 2012)S

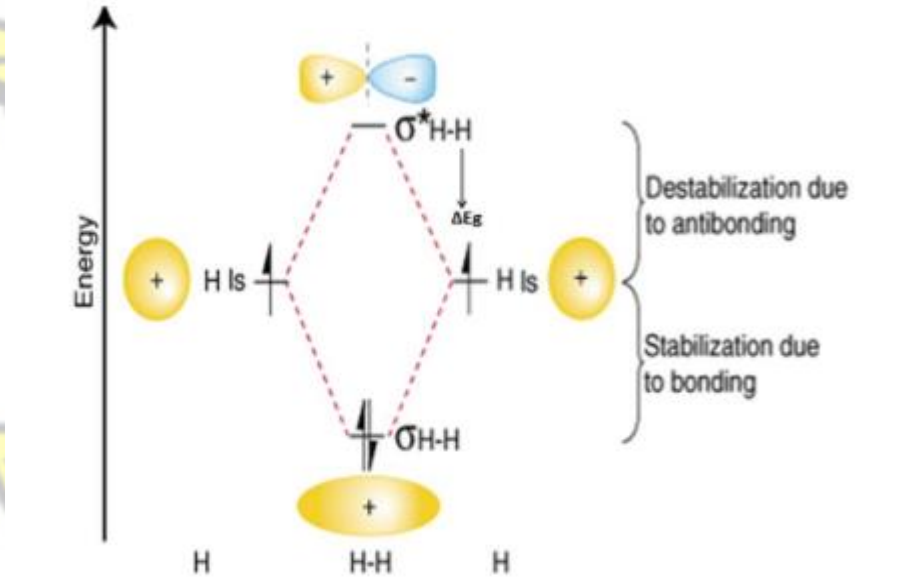


Figure 2.1 Molecular orbitals in a diatomic molecule.

The valence band (VB) represents the highest occupied molecular orbital (HOMO) and the conduction band (CB) represents the lowest unoccupied molecular orbital (LUMO). The gap between the highest filled energy level and lowest unfilled energy level is called band gap (Eg). These are delocalized over both atoms, and the bonding molecular orbital possess lower energy than the $H_1$ and $H_2$ atomic orbital, while the antibonding molecular orbital has higher energy. The energy band that results from the bonding orbitals of a molecule is known as the valence band, while the conduction band is because of the antibonding orbitals of the molecule. The width of individual bands across the range of energy levels is called band width. The valence band (VB) represents the highest occupied molecular orbital (HOMO) and the conduction band (CB) represents the lowest unoccupied molecular orbital (LUMO). The gap between the highest filled energy level and lowest unfilled energy level is called band gap (Eg). This band gap represents a range of energies which is not available to electrons, and this gap is known variously as 'the fundamental energy gap', the 'band gap', the 'energy gap', or the 'forbidden gap. The level of electrons in a system which is reached at absolute zero is called the Fermi level (Fg) (Daintith and Martin, 2010). It has been demonstrated that in order to allow the formation of delocalized electronic states, CPs molecular arrangement must be conjugated. The delocalization of the electronic states relies on the resonance stabilized structure of the polymer. The size of the energy band gap depends on the extent of delocalization and the alternation of double and single bonds (Cheng et al., 2009). Moreover, the size of the energy band gap will determine whether the CP is metal, semiconductor or insulator.

### 2.2.2 CONDUCTION MECHANISM IN POLYANILINE

The electrical conductivity of a material is mainly determined by its electronic structure. (Le et al., 2017). The primary requirement for a polymer to be conductive is that it must have a conjugation in the chain backbone for easy movement of charge carriers For PANI there are single and double bonds that makes it a conjugated polymer but that does not make the polymer conductive unless intrinsic charge carriers are developed. Once the charge carriers are generated, the band gap is reduced and the system becomes conductive. This is because the charge carriers are provided with

extrinsic charge transfer process (partially oxidation or partially reduction with appropriate agents). This process in conducting polymers is now as doping.

Doping of polymers may be done with several techniques such as

(a) Gaseous doping

(b) Solution doping

(c) Electrochemical doping

(d) Self-doping

(e) Radiation doping



Unlike metals where there are free spins for its charge carriers regarding their conductivity, conducting polymers as stated earlier have charge carriers without free spins. During donor or acceptor molecule to a conjugated polymer the reaction which takes place is a redox reaction. This is quite different from the doping of metals such as silicon and germanium where substitution of atoms takes place in the lattice. Doping in conducting polymers like PANI involves the formation of polymer salt and this happens either by exposing the polymer to the dopant in a solution or by electrochemical process. The reaction is given below:

$$P \xrightarrow[X^+A^-]{\text{Oxidation}} P{:}X^+/A^- \qquad \text{p-type} \qquad (1)$$

$$P \xrightarrow[X^+A^-]{\text{Reduction}} P{:}A^-/X^+ \qquad \text{n-type} \qquad (2)$$

Where P represents a section of the polymer chain. First a cation or anion radical is created and this is called a soliton or polaron. In the case of PANI the radical created is a polaron. This is

followed by a second electron transfer with the formation of a dication or dianion known as bipolaron. The polarons and bipolarons are mobile under the influence of electric field and can transport along the chain. The conduction mechanism is known to involve polaronic carriers (protonated emeraldine which consist of a delocalized poly (semiquioione radical cation)). The basic form of polyaniline (A) contains benzenoid and quinoid rings in the ratio of 3:1. This is diamagnetic and insulating and its paramagnetic centers and conductivity appear after doping. Doping results in the appearance of positively charged paramagnetic polarons and diamagnetic bipolarons two polarons (C) can recombine to form one bipolaron (B). Conductivity can be as results of motions of both polarons and bipolarons (Kulikov et al., 2002). Bipolarons prevail in polyaniline salt nevertheless conductivity occurs mainly through jumps of polarons both along the polymeric chain and between the chains.

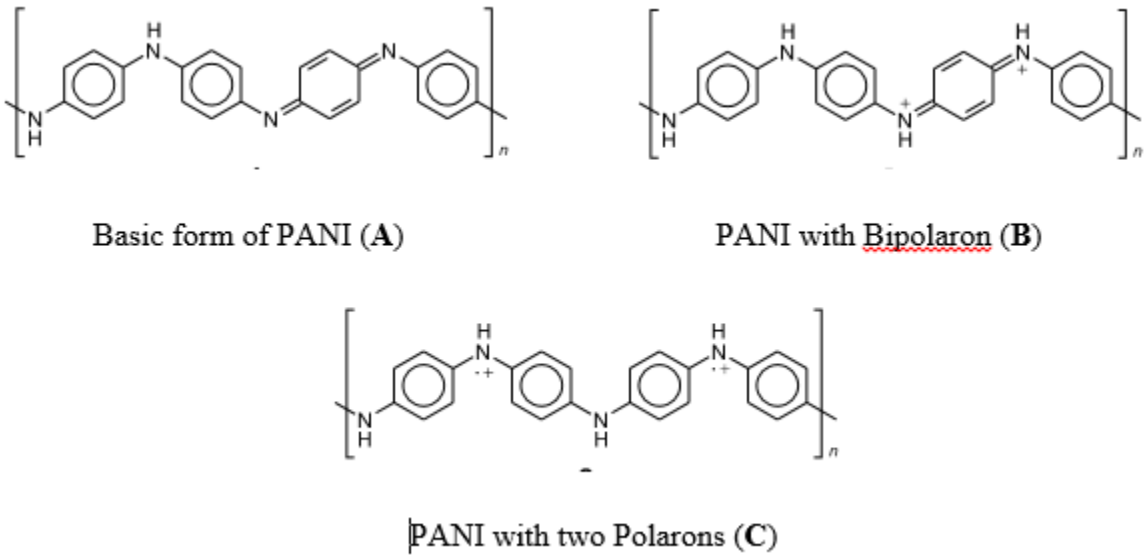


Figure 2.2 Different forms of PANI with Polarons and Bipolarons

The presence of nitrogen in the conjugated path of PANI chain provides a way to dope PANI through non-redox routes and this has significant influence on the nature of quasi-particles

which are responsible for charge transport. Oxidative doping can be carried out by reacting PANI with an acid (nitric acid ($HNO_3$), hydrochloric acid (HCl), Sulfuric acid ($H_2SO_4$)) and others that tend to pull out lone-pair of electrons from the double-bonded imine N atoms and thereby creating vacancies in the $\pi$-electron cloud (34-37). This converts the imine sites to iminium (an imine with positive charge) sites. PANI can also be doped with organic dopants such as acetic acid ($CH_3COOH$), camphor sulfuric acid (CSA) etc. The doped samples can also be electrically nuetralised or dedoped. This process is reversible as doping or dedoping of PANI is done by exposing the polymer to acid and base respectively. The electronic state of can also be altered via electrochemical diffusion of dopant ions in the polymer. This is done by applying a proper voltage between two electrodes through a potential loading device to cause a reverse electrode reaction in the electrolyte solution.

## 2.3 EXPERIMENTAL TECHNIQUES

### 2.3.1 Synthesis of polyaniline (PANI)

Polyanilines are probably the most rapidly growing class of conducting polymers as can be seen from the number of papers and patents (1237) published during the last five years, 2 ) viz., 1986 (108); 1987 (221); 1988 (236); 1989 (383); 1990 to June 3, 1991 (289). These figures are due in large part to the very considerable industrial interest in the polyaniline (MacDiarmid et al., 1987).

Oxidation of aniline is the most widely employed synthetic route to polyaniline (Boeva et al.,2014). Polyaniline has an added advantage of being easily synthesized or prepared from

common chemicals such as Hydrochloric acid (HCl) or sulfuric acid ($H_2 SO_4$) being used as a dopant for inducing the formation of an emeraldine salt (ES) that can be performed via the chemical or electrochemical polymerization of aniline in the presence of dopants (acidic medium) with a chemical oxidizing agents such as ammoniumpersulfate.

Depending on the synthesis procedure; the temperature and time regimes; the types of oxidant, dopant, and solvent; the voltage applied on the electrode; etc., polyaniline featuring different properties namely, the structure, morphology, and redox state may be prepared (Heeger, 2001). As stated earlier the emeraldine salt (ES) is the most conducting form of PANI. The emeraldine base (EB) can be conducting when protonated using the acidic medium. Similarly, the ES can be converted to base (suggestion: 'base form') by adding $NH_4OH$ solution to it. Bulk samples of PANI can be obtained after drying or during the oxidation precipitation as films on substrates, as layers on a support.

### 2.3.2 **Chemical Oxidative Synthesis**

Bulk samples of PANI can be prepared by using the chemical oxidative polymerization method. For chemical polymerisation to take place monomers have to be oxidized to initiate the reaction. Synthesis of PANI by chemical oxidation way involves the use of hydrochloric acid, sulfuric acid and other kinds of acids in the presence of ammonium persulfate as the oxidizing agent in the aqueous medium. Also, ammonium per sulphate happens to be the commonest oxidant used, but there are several others, including some very common ones, like hydrogen peroxide and potassium per sulphate. The main function of the oxidant is to withdraw a proton from an aniline molecule, without forming a strong co-ordination bond either with the substrate / intermediate or with the final product. Polymer chains proceed by a redox process between the growing chain and aniline with addition of monomer to the chain end. The high concentration of a strong oxidant,

$(NH_2)_2S_2O_8$, at the initial stage of the polymerization enables the fast oxidation of oligomers and polyaniline, as well as their existence in the oxidized form (Bavane, 2014).

Chemical synthesis requires three reactants: aniline, an acidic medium (inorganic or organic) and an oxidant. The more popular synthesis is to use 1 mol aqueous acid solution, ammonium persulfate as oxidant with an oxidant/aniline molar concentration ratio of $\leq 1.15$ in order to obtain high conductivity and reduce wastage of monomer (Syed et al., 1991). The solution temperature may be set between 0 and 2°C in order to limit secondary reactions. The duration of the reaction varies generally between 1 hr and 2 hr. The experimental part consists of adding slowly (drop by drop) the aqueous ammonium persulfate solution to the aniline/acid. The mixture is stirred for about 1 hr. The obtained precipitate is removed by filtration and washed repeatedly with the acidic medium and dried under vacuum for 48 hr. The obtained material is polyemeraldine salt: polyemeraldine hydrochloride (PANI-HCl). To obtain polyemeraldine base, polyemeraldine hydrochloride is treated in an aqueous in either potassium hydroxide or sodium hydroxide solution. The obtained powder is washed and dried (Bavane, 2014).

### 2.3.4 Electrochemical Oxidative Synthesis

It is possible to synthesize polyaniline by the electrochemical oxidation of aniline in aqueous acidic media on conducting glass electrodes (e.g. ITO) as thin films. Electrochemical synthesis involves oxidation or reduction of the monomer species in electrolyte solutions to obtain usually compact films directly on the electrode (Wagner, 2013). In most of the applications of conducting polymers, it is essential to synthesize polymers as thin films of well-defined structure. For preparation of such films, electrochemical synthesis is a standard method (Bavane, 2014). It is best to use the electrochemical method for conducting polymers which are not so easy to process

using the chemical oxidative method. The electrochemical synthesis of conducting polymers is similar to the electrodeposition of metals from an electrolyte bath; the polymer is deposited on the electrode surface and also in the in-situ doped form. There is the three-electrode system and the two-electrode system. The three-electrode set-up comprises of a working electrode on which the polymer is deposited, a counter electrode and a reference electrode. The most common working electrode is a platinum one, but PANI depositions have also been made on conducting glass (glass covered by indium-doped tin oxide (ITO) electrode), Fe, Cu, Au, graphite, stainless steel, etc. (Syed et al., 1991). PANI can be then peeled off from the electrode surface by immersion in an acidic solution. The electrochemical synthesis is normally carried out in a single compartment cell.

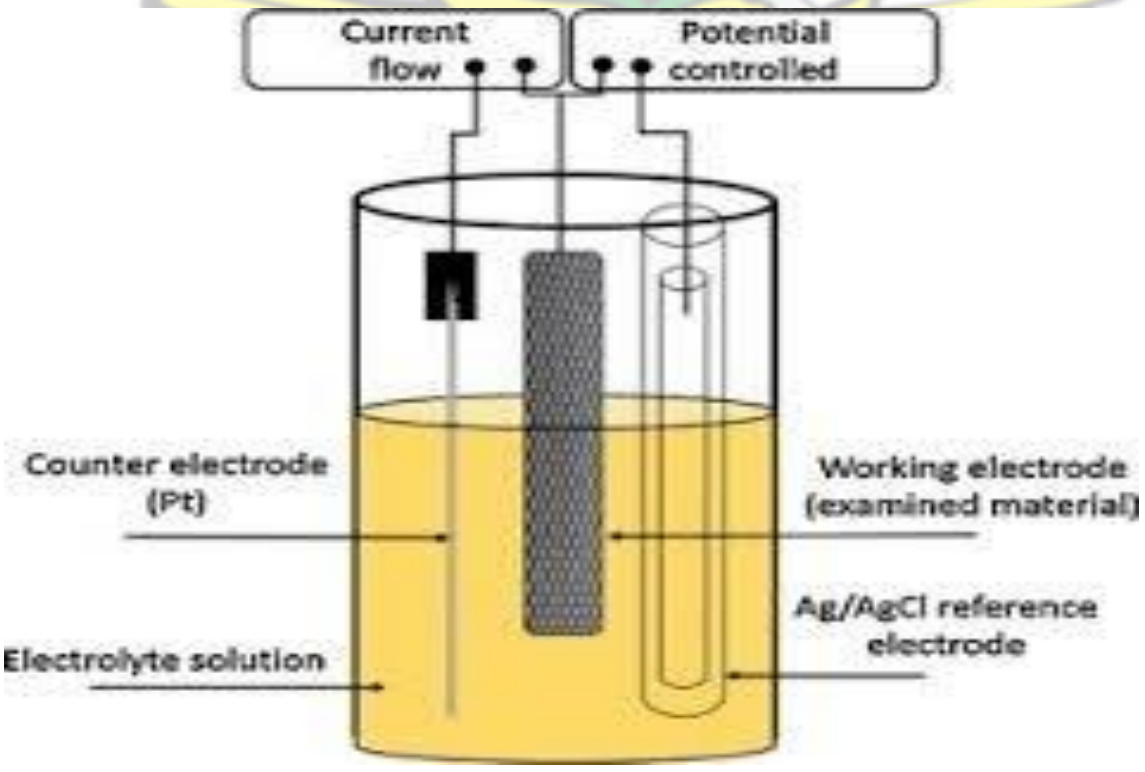


**Figure 2.3: Schematic set-up for electrochemical deposition on ITO glass slide**

The cell consists of the electrodes, electrolyte and power supply. Electrochemical polymerization has many advantages over chemical synthesis of PANI, such as strict control of the oxidation potential applied during synthesis providing the unique ability to moderate the polymerization initiation and termination processes (Bhadra et al., 2007). Also, there is cleanness because no extraction from the monomer–solvent–oxidant mixture is necessary, doping and thickness control via electrode potential, simultaneous synthesis and deposition of PANI thin layer.



There are other advantages electrochemical oxidative method has over chemical oxidative method. These are:

1. It is simple and less expensive technique. Therefore, electrodeposition of conducting polymer on conducting glass is extremely economical.
2. Unlike chemical method, there is no need for catalyst and therefore, the electrodeposited polymers and co-polymers are essentially pure and homogeneous.
3. The conducting polymers can be obtained directly in thin film forms as coating on electrodes and the properties of these coatings can be controlled effectively by proper choice of the electrochemical process variables.
4. Reduction in the possible pollution by adopting the suitable system for electropolymerization using modern sophisticated instrument.

## 2.4 Characterization Techniques

### 2.4.1 UV-Vis-NIR Spectroscopy

Ultraviolet–visible spectroscopy or ultraviolet-visible spectrophotometry (UV-Vis or UV/Vis) refers to absorption spectroscopy or reflectance spectroscopy in the ultraviolet-visible spectral region. This means it uses light in the visible and adjacent ranges. The absorption or reflectance in the visible range directly affects the perceived colour of the chemicals involved. The absorption of ultraviolet or visible radiation by a molecule leads to transitions among the electronic energy levels of the molecule. It is ideal for characterizing the optical and electronic properties of various materials such as: films, powders, monolithic solids, and liquids (Skoog et al., 2017). Measurements in the ultraviolet/visible region (UV-VIS) cover wavelengths from about 200 nm to 800 nm. In this region of the electromagnetic spectrum, atoms and molecules undergo electronic transitions. Absorption spectroscopy is complementary to fluorescence spectroscopy, in that fluorescence deals with transitions from the excited state to the ground state, while absorption measures transitions from the ground state to the excited state. Molecules containing $\pi$-electrons or non-bonding electrons (n-electrons) can absorb energy in the form of ultraviolet or visible light to excite these electrons to higher anti-bonding molecular orbitals. The more easily excited the electrons (i.e. lower energy gap between the HOMO and the LUMO), the longer the wavelength of light it can absorb. Also, the absorbance of a solution is directly proportional to the concentration of the absorbing species in the solution and the path length. Thus, for a fixed path length, UV/Vis spectroscopy can be used to determine the concentration of the absorber in a solution. The absorbance changes with concentration.

The data that UV-Vis spectroscopy gives, when combined with the information provided by other spectral data such as (infrared) IR and (Nuclear Magnetic Resonance) NMR leads to valuable structural data. Atoms and molecules exist in a number of defined energy states or levels and a change of level requires the absorption or emission of an integral number of a unit of energy called a quantum of energy a photon. The energy of a photon absorbed or emitted during a transition from one molecular energy level to another is given by the equation:

$$E = h\nu \qquad (2.1)$$

Where h is known as Planck's constant and $\upsilon$ is the frequency of the photon.

$$c = \upsilon\lambda \qquad (2.2)$$

Therefore,

$$E = hc/\lambda \qquad (2.3)$$

A molecule of any substance has an internal energy which can be considered as the sum of the energy of its electrons, the energy of vibration between its constituent atoms and the energy associated with rotation of the molecule. The electronic energy levels of simple molecules are widely separated and usually only the absorption of a high energy photon, that is one of very short wavelength, can excite a molecule from one level to another. The UV-Vis spectrophotometer operates by passing a beam of light through a sample and measuring wavelength of light reaching a detector. The wavelength gives valuable information about the chemical structure and concentration in the sample. Analytical information can be revealed in terms of transmittance, absorbance or reflectance of energy in the wavelength range between 160 and 3500 mμ Light is quantized into tiny packets called photons, the energy of which can be transferred to an electron upon collision. However, transfer occurs only when the energy level of the photon equals the energy required for the electron to be excited to a designated higher energy

state of the atom or molecule, for example from the ground state to the first excitation state. This process is the basis for absorption spectroscopy.

Generally, light of a certain wavelength and energy is illuminated on the sample, which absorbs a certain amount of energy from the incident light. The energy of the light transmitted from the sample afterwards is measured using a photo detector, which registers the absorbance of the sample. A spectrum is a graphical representation of the amount of light absorbed or transmitted by matter as a function of wavelength (Sibilia, 1996). Bouguer–Beer law is a basic principle of quantitative analysis, is also called the Lambert–Beer rule. The following relationship is established when light with intensity $I_o$ is directed at a material and light with intensity I is transmitted.

The value $\log \frac{1}{T} = \log \frac{Io}{I}$ is called absorbance (Abs). (2.4)

$$T = \frac{I}{Io} = 10^{-kcl} \quad (2.5)$$

$$\text{Abs} = \frac{1}{T} = \log \frac{Io}{I} = -kcl \quad (2.6)$$

Where k is proportionality constant and l is length of light path through the cuvette in cm. From the above formulas, transmittance is not proportional to sample concentration. However, absorbance is proportional to sample concentration (Beer's law) along with optical path (Bouguer's law). In addition, when the optical path is 1 cm and the concentration of the target component is 1 mol/l, the proportionality constant is called the molar absorption coefficient. The molar absorption coefficient is a characteristic value of a material under certain, specific conditions. Finally, stray light, generated light, scattered light, and reflected light must not be

present for the Bouguer–Beer rule to apply (Sibilia, 1996). An absorption peak at around 380 nm is attributed to the charge transfer corresponding to transition of aromatic ring.

There is a peak around 270 nm, which is attributed to a transition involving non-bonding electrons from the bonding band to other anti-bonding orbitals. For example, from the non-bonding electron orbital to the anti-bonding orbital in the aromatic ring, $p \rightarrow p^*$, the first absorption band of p–p * bond appears at 280–295 nm and it is assigned to the p–p * transition of the benzenoid ring on the basis of the earlier studies on polyaniline (Tzou et al., 1993) and it is related to the extent of conjugation between the adjacent phenyl rings in the copolymer chain. The second absorption band located at 605–635 nm is attributed to the quinoid ring transition (charge transfer from HOMO of the benzenoid ring to LUMO of the quinoid ring) (Tzou and Gregory, 1993). The absorption spectrum of the polyaniline salt doped with HCl shows bands at 326, 433 and 630 nm, with higher conductivity (Yang and Mu, 2008). A characteristic band for polaron-p * transition appeared at 450 nm, indicating that the resulting PANI emeraldine salt was in the doped state (Razak et al., 2009).

### 2.4.2 FTIR Spectroscopy

An easy way to identify the presence of certain functional groups and to confirm the presence of particular bonds in the sample in a molecule is to use FTIR spectroscopy. Also, one can use the unique collection of absorption bands to confirm the identity of a pure compound or to detect the presence of specific impurities. Analysis by infrared spectroscopy is based on the fact that molecules have specific frequencies of internal vibrations. These frequencies occur in the infrared region of the electromagnetic spectrum ~ 4000 $cm^{-1}$ to ~ 200 $cm^{-1}$. Identification of a substance is possible because different materials have different vibrations, yield different

infrared spectra and different chemical compositions. Furthermore, from the frequencies of the absorption it is possible to determine whether various chemical groups are present or absent in a chemical structure. In addition to the characteristic nature of the absorption, the magnitude of the absorption due to a given species is related to the concentration of that species (Sibilia, 1996).



There are specific bands that are characteristics of polyaniline. The band at 3380 $cm^{-1}$ corresponds to the N-H vibrations of PANI (Sariciftci et al., 1987). The bands at 3274 and 3051 $cm^{-1}$ in the spectrum of a PANI base are attributed to hydrogen-bonded N–H stretching (Kang et al., 1998) (Sedˇ enkovˇ a et al., 2006) (Stejskal et al., 2008). A broad absorption band´ at wavenumbers higher than 2000 $cm^{-1}$ in the spectrum is due to the absorption of free charge-carriers in the protonated polymer (Neoh et al., 1993) (Ping, 1996). A shoulder observed at 1610 $cm^{-1}$ in the spectrum is characteristic of C=C ring vibrations in the polymer chains whose symmetry has been broken by conformational changes induced by protonation. The bands at 1577 and 1482 $cm^{-1}$ due to quinonoid (Q) and benzenoid (B) ring-stretching vibrations, respectively, observed in the spectrum (protonated salt form) (Ping, 1996). The band characteristic of the conducting protonated form is observed at 1248 cm $cm^{-1}$ in the spectrum. It has been interpreted as corresponding to a C–N +• stretching vibration in the polaron structure (Ciri c-Marjanovic et al., 2008).

The spectrum exhibits a strong and broad band centered at 1148 cm $cm^{-1}$ , which has been assigned to the vibration mode of the –NH + = structure, and is associated with the vibrations of the charged polymer units Q=NH + B or BNH +• B (Trchova and Stejskal, 2011). This indicates the existence of positive charges on the chain and the distribution of the dihedral angle between the quinonoid and benzenoid rings. The absorption band increases with increasing degree of

protonation of the PANI backbone (MacDiarmid and Chiang, 1986). The band at 882 $cm^{-1}$ in the spectrum can be attributed to the $HSO_4^-$ counterion, which was removed during the deprotonation (Lin-Vien et al., 1991). The band observed at 760 and 695 cm−1 in the spectrum corresponds to the C–H out-of plane bending (Trchova et al., 2006).



### 2.4.3 **Cyclic Voltammetry**

Voltammetry is any experiment where we expose a solution of an analyte to an electrode, change the electrode potential, and observe the current that flows in response. Cyclic voltammetry is generally used to study the electrochemical properties of an analyte in solution or of a molecule that is adsorbed onto an electrode (Trojanowicz et al., 2006).

In cyclic voltammetry, the electrode potential ramps linearly versus time in cyclical phases. The current is measured between the working electrode and the counter electrode while the potential is measured between the working electrode and the reference electrode. The current (i) is plotted against the applied potential. The utility of cyclic voltammetry is dependent on the analyte being studied. The analyte has to be redox active within the potential window to be scanned. CV experiments are conducted on a solution in a cell fitted with electrodes. The solution consists of the solvent, in which is dissolved electrolyte and the species to be studied. Cyclic Voltammetry can be used to study qualitative information about electrochemical processes under various conditions, such as the presence of intermediates in oxidation-reduction reactions and, the reversibility of a reaction (Dryhurst et al., 2012).

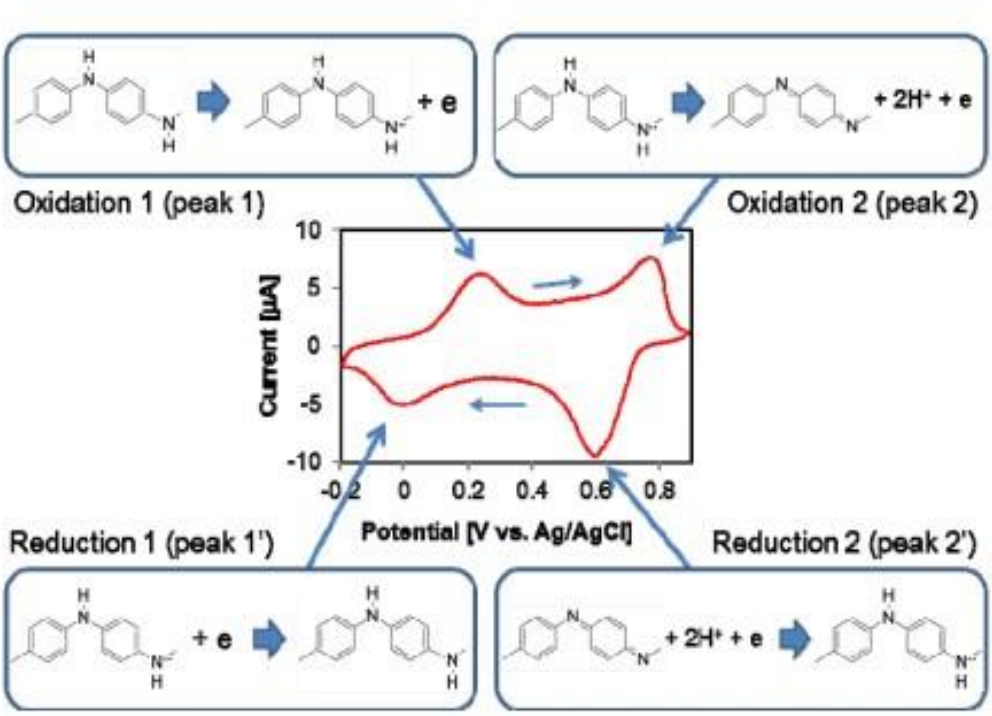


Figure 2.4: Cyclic Voltammogram of PANI at potential of 0.8 V

For analyte which is redox–active (aniline + aqueous acid), it will exchange an electron with an electrode when it reaches certain potentials. The redox–active analyte will undergo reduction (accept an electron from the electrode) when the potential energy of the electrons in the electrode is higher than the potential energy of the empty molecular orbital on the analyte so it is energetically favorable for an electron to transfer from the electrode to the analyte. Conversely, the analyte will undergo oxidation (losing an electron to the electrode) when the highest energy electron in the molecule is at a higher potential energy than the electrons in the electrode, and it becomes energetically favorable for it to transfer from the molecule to the electrode. In both of these cases, electrons are transferred in order to minimize the potential energy of the total system.

We can use the potentiostat to change the electrode potential and observe where we see current flowing in order to learn about the electron transfer energetics of our analyte.



### 2.3.4 Thin Film Thickness Measurements Techniques

Thin films are layers of materials with thicknesses ranging from a few atoms to microns. The main uses are for optical coatings, semiconductor devices and thin film photovoltaic devices. In most cases, the thickness of the film is carefully monitored and controlled so that the final product may function properly. This can be done by a number of methods, but optical techniques are preferred as they are non-contact, non-destructive, fast and accurate. To make sure that coatings which were produced by a given process satisfy the specified technological demands a wide field of characterization, measurement and testing methods is available. The physical properties of a thin film are highly dependent on their thickness. The determination of the film thickness and of the deposition rate therefore is a fundamental task in thin film technology. In many applications it is necessary to have a good knowledge about the current film thickness even during the deposition process, as e. g. in the case of optical coatings. Therefore one distinguishes between thickness measurement methods which are applied during deposition (”in situ”) and methods by which the thickness can be determined after finishing a coating run (”ex situ”). There are several techniques used in measurement of the thickness of thin films. We have the Gravimetric method, Optical method, Direct method etc

**Gravimetric Method**

These methods are based on the determination of a mass. The film thickness d can be calculated from the mass of the coating m if the density $\rho$ and the area A on which the material is deposited are known:



$$d = \frac{m}{A\rho} \tag{2.7}$$

For this method one must bear in mind that the density of a coating may deviate significantly from that of the bulk (e.g. due to porosity or implanted interstitial atoms). For exact measurements calibration is necessary. The weighing under this method which is the simplest method for film thickness determination is most probably the determination of the mass gain of coated substrate with an exact balance. (Owusu-Sekyere *et al.,* 2017). The difference in the mass is related to the density of the material deposited and with that relation the volume which has the height of the deposited material can be re-arranged to obtain the thickness of the material. Taking into the consideration the measurement of the area of the sample on the substrate.

**Optical Method**

Optical coatings, unlike other applications, require the measurement of the film thickness as exactly as possible during deposition. Therefore, film thickness monitors are used which, especially in the case of multi coated optics (interference filters etc.) are incorporated into closed loop controls by (in some cases quite complex) software components. There is Photometer Method mostly used in Physical Vapor Deposition (PVD) processes for the production of single

layer and multiplayer coatings for optical applications. It measures the optical thickness and so that it allows for a compensation of changes in the refractive index by corresponding changes of the film thickness. First is the Tolansky interferoneter, a film thickness can be determined by this method as follows: First a scratch is made into the film which reaches down to the substrate (it is also possible to mask a part of the substrate during deposition which leads to the formation of a step). Then the sample is coated by a highly reflective layer. Because of the scratch the distance reflector/interference slide is changed, which leads to an offset of the interference lines relative to each other. The films thickness is given by:

$$d = \frac{\Delta N \Delta}{2} \tag{2.8}$$

Where Δ N is the number (or the part) of the lines by which the interference lines are shifted by the scratch or the step. Next is Fringes of Equal Chromatic Order (FECO) method, parallel white light is illuminating the combination of sample and reference slide. The reflected light is focused into the entrance slit of a spectrograph via a semitransparent mirror. The image of the step has to be normal to the entrance slit. Dark interference lines are observed at the wavelengths.

$$\lambda = \frac{2t}{N} \tag{2.9}$$

Where t is the thickness and N is the interference order . Other methods under the optical methods include; Nomasky interferometer and Ellipsometry.

### 2.4.5 Electrical Conductivity Measurements

In chemical bonding of materials is mostly indicated by the electrical resistivity measurements. The change in the nature of the chemical bonding alters the carrier density which is inversely

proportional to the carrier mobility (Singh, 2013). The electrical conductivity of the material is also inversely proportional to the electrical resistivity. There is therefore the need to first determine the electrical resistivity of the material before calculating the material's electrical conductivity. To do this there are two known techniques that are employed in determining the electrical resistivity/electrical conductivity of a material. They are the two (2) probe method and the four (4) probe method.



**2-Point Probe**

The two probes (ohmmeter or voltmeter – ammeter measurements) is one of the simplest methods of measuring the electrical resistivity and can be used for higher resistive samples. The figure below shows the two-point probe set-up. According to the diagram below voltage drop V across the sample and current through the sample I are measured. Then the resistivity is given as:

$$\rho = \frac{V\,A}{I\,L} \qquad (2.10)$$

Where L is the length of the sample and A is the cross-sectional area of the sample.

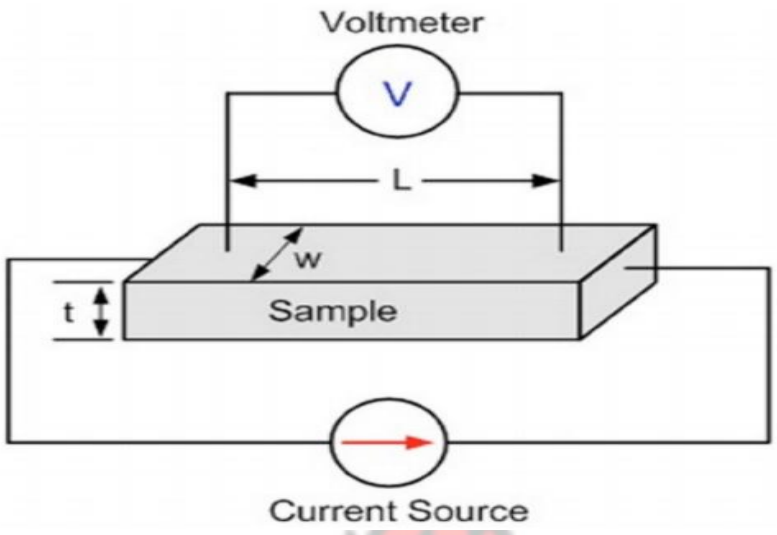


**Figure 2.5: Circuit diagram for Two-point probe on a Sample**

**4-Point Probe**

The potential probe is the most widely used method for resistivity measurements on the low resistive samples. The diagram below represents the entire set–up for the four point probe.

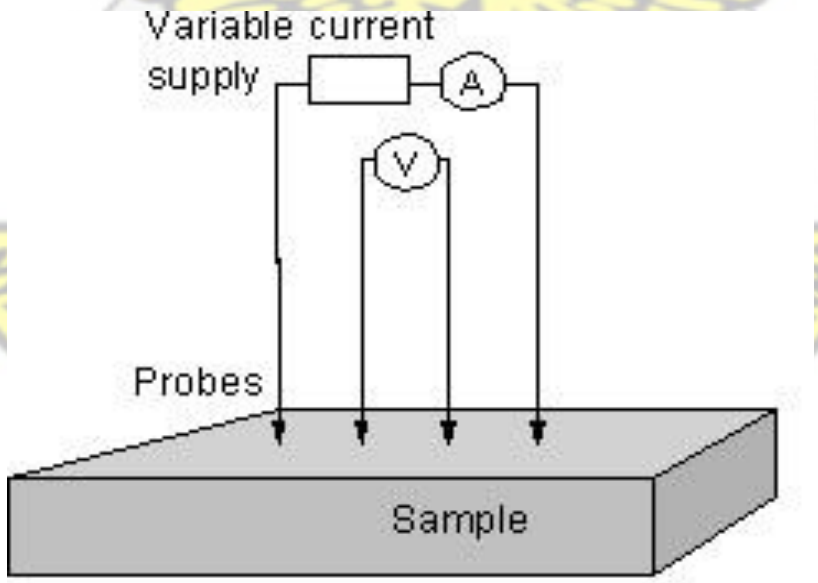


**Figure 2.6: Circuit diagram for Four-point probe on a Sample**

The potential drop is measured across two probes and distance between these probes D replaces the sample length L in equation 2.10. When the probes are not point contacts, in that case, the most accurate value for the probe distance is the distance between the centers rather than the closest distance between the probes. The equation is given by:

$$\rho = \frac{V\,A}{I\,L} \qquad (2.11)$$

The 'four-point probe' method has proven to be a convenient tool for the resistivity measurement of small size (of the order of mm) samples (Singh, 2013).

# CHAPTER 3

# METHODOLOGY

## 3.1 Synthesis of Polyaniline (PANI)



### 3.1.1 **Polymerization Process (Chemical Oxidation)**

12.03 g of $(NH_2)_2S_2O_8$ was measured and put in 600 ml beaker. 5.00 g of the aniline monomer was measured into a 500 ml beaker. Ammonium persulphate solution (APS) was formed by adding 70 ml of $H_2SO_4$ to it. 75 ml of $H_2SO_4$ was poured into the aniline monomer. Drop-wise addition of aniline to the APS solution was done. Change in the colour of the solution was observed after 10 minutes. The colour of the solution changed from brown-whitish to pale green then green (emeraldine salt). The solution was left for 12 hours for complete polymerization to occur.

The oxidant, 12.0 g , was measured into 600 ml beaker. A mass of 5.01 g of aniline monomer was measured into a 500 ml beaker. The aqueous acid used this time was $HNO_3$. An APS solution was formed, and the aniline solution was poured drop-wise into it. In less than a minute the colour change of the solution was observed. A pale green and then a green dark solution was formed. The polymer was left for 12 hours at room temperature for complete polymerization to take place.

Using the 1 M HCl prepared, 12.38 g of the oxidant was used to prepare the APS solution. 5.05 g of the aniline monomer was measured and the aniline solution formed with 75 ml of the HCl. The aniline solution was poured into the APS solution drop-wise. There was an immediate colour change when the aniline solution was added to the APS solution. For complete polymerization the

solution was left for 12 hours. The same amount of oxidant 12.0 g was measured into 600 ml beaker. A mass of 5.01 g of aniline monomer was measured into a 500 ml beaker. The aqueous acid used this time was $CH_3COOH$. An APS solution was formed and the aniline solution was poured drop-wise into it. A pale green and then a dark green solution were formed. The polymer was left for 12 hours at room temperature for complete polymerization to take place. Each of the Emeraldine salt formed was filtered by continuously washing with the acid until the filtrate was clear. The samples were dried at 70 °in an oven and crushed into powder form. For each sample, some of the powder was hard pressed into pellet using a metallic mold.

### 3.1.2 **Electrochemical Oxidation Using Different Dopants**

75 ml of 1 M of the HCl was measured into 100 ml beaker. Volume of 5 ml of the aniline was poured into the aqueous acid and stirred for 10 minutes to acquire a uniform solution. The three electrodes (ITO (working), Platinum (counter) and Ag/AgCl (reference)) were placed into the solution to form a single cell compartment and connected to the potentiostat. A potential of 0.7 V was applied for deposition to be completed in 10 minutes for each sample. The samples were dried at 60°C for 30 minutes. The entire steps were repeated for all the other acids used.

## 3.2 **CHARACTERISATION OF SAMPLES**

### 3.2.1 **FOURIE TRANSFORM INFRARED SPECTROSCOPY (FTIR)**

The bulk samples and thin films were taken to the Central Lab-KNUST for FTIR results using an OPUS software along with the BRUKER and PerkinElmer Spectrum Version 10.03.09. Each

sample was placed on the sample holder and a probe was adjusted to make contact with the sample. Using the OPUS software, the spectrum for the T% against $cm^{-1}$ for each sample was obtained.

### 3.2.2 **ULTRAVIOLET-VISIBLE SPECTROCOPY (UV-Vis)**

The thin film samples were placed into the sample holder for cuvette and the HyperThermal Software was used to run a complete spectrum from 200 nm to 1200 nm. A solution of the powered samples was made and poured into a cuvette before a complete spectrum was run for the bulk samples. A spectrum of the absorbance against the wavelength of each sample was obtained.

### 3.2.3 **CYCLIC VOLTAMMETRY**

2.309 g of aniline was measured, and 0.05 ml of distilled water was added to it. The solution was stirred under a magnetic stirrer for 5 minutes. A 0.05 ml of the 1 M HCl solution was added to the aniline solution. This was stirred for 5 minutes to obtain uniform solution. The three electrodes (working, counter and reference) were placed into the solution and connected to the potentiostat. A potential of 0.7 V was applied for deposition to be completed in 10 minutes for each sample. Cyclic voltammetry technique was selected from the interface using the EChem v2.1.12 software. The following parameters were used to perform the cyclic process. Scan rate of 100 mV/s, Step width of 20 ms, 1 cycle and rest time of 2 seconds were used. The procedure above was repeated for the other dopants. A graph of I/mA and V/mV was obtained.

### 3.2.4 **CONDUCTIVITY**

The thin film samples were placed in a sample holder and the four-probe adjusted to contact the sample surface. An appropriate current ranging from (0.20 -5.00) mA was applied and the corresponding voltage in mV was recorded for the samples. For the bulk samples, the pellets were placed in the sample holder and appropriate current within the range of 0.22 - 4.50 mA were applied and their corresponding voltages measured in mV.



# CHAPTER 4

# RESULTS AND DISCUSSION



## 4.1 FOURIER TRANSFORMATION INFRARED SPECTROSCOPY (FTIR)

To analysis the various functional groups present in the synthesized samples, a FTIR spectroscopy was carried out using BRUKER EQUINOX-55 and PerkinElmer Spectrum Version 10.03.09. Below are the results of the IR of the different samples.

### FTIR of Thin Films

The most dominant bands in the entire spectra which are clear characteristics of polyaniline were 3468 $cm^{-1}$ – 3025.17 $cm^{-1}$, 1593 $cm^{-1}$ – 1553 $cm^{-1}$, 1481 $cm^{-1}$ – 1413 $cm^{-1}$, 1300 $cm^{-1}$ – 1239 $cm^{-1}$, 1142 $cm^{-1}$ -1022 $cm^{-1}$ and 883 $cm^{-1}$ – 880 $cm^{-1}$. Below is a table for the various peaks recorded for the thin film samples.

Table 4.0 Fourier Transformation Infrared Spectroscopy of the Thin Film Samples

| SAMPLE | N-H stretching | C-H stretching | C = N stretching | Quinoid Bond | Benzenoid Bond | C-H out of plane |
|---|---|---|---|---|---|---|
| HCl | - | - | 1670 | 1561 | 1481 | 787 |
| $H_2SO_4$ | - | - | 1650 | 1561 | 1478 | 789 |
| $HNO_3$ | 3468 | 3266 | 1673 | 1563 | 1500 | 827 |
| $CH_3COOH$ | 3384 | 3050 | - | 1553 | 1481 | 820 |

Wavenumbers higher than 2000 $cm^{-1}$ are due to the absorption of free charge-carriers in the protonated polymer and that is a characteristic of a conducting form of polyaniline.

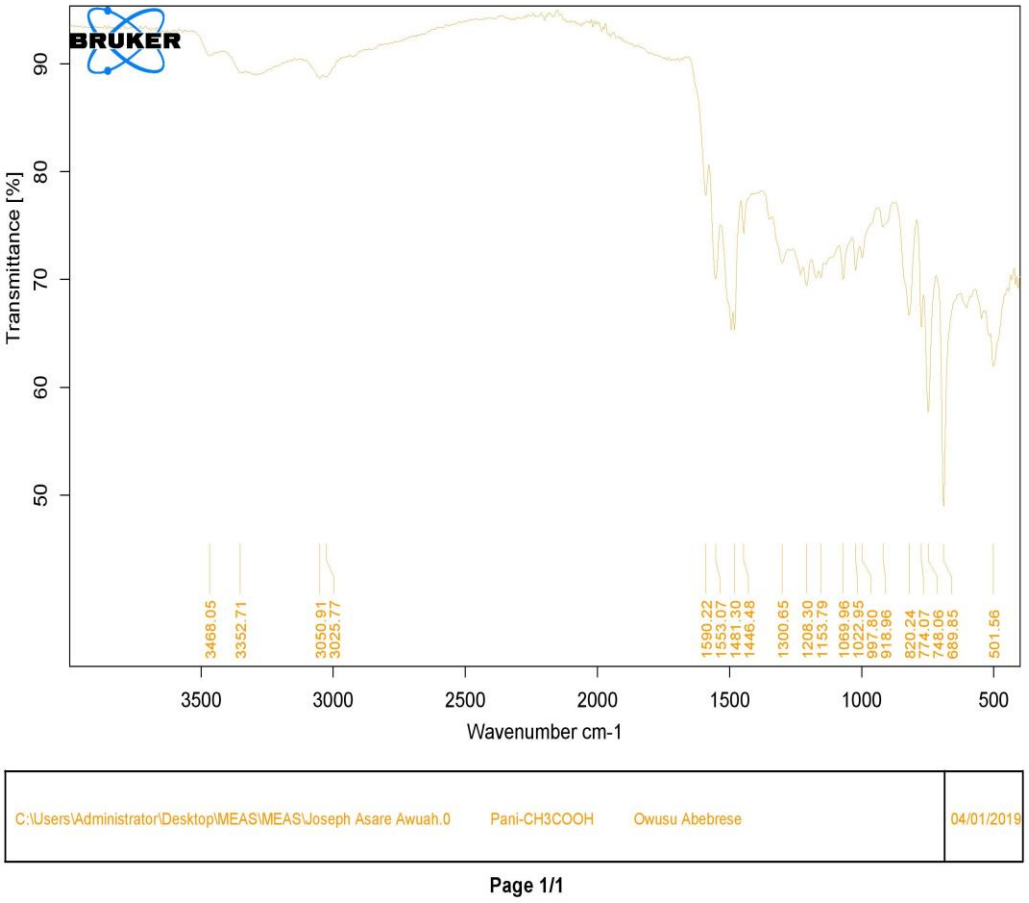


**Figure** 4.1: FTIR of PANI-$CH_3COOH$ thin film

At 1670 $cm^{-1}$ and 1673 $cm^{-1}$ for PANI-HCl and PANI-$HNO_3$ respectively there is a C=N stretching mode of the imine. The quinoid (Q) stretching vibrations appear at the 1563 $cm^{-1}$ band for the PANI-$HNO_3$ but I the PANI-$CH_3COOH$ it appears at the 1553 $cm^{-1}$ band. The quinonoid ring

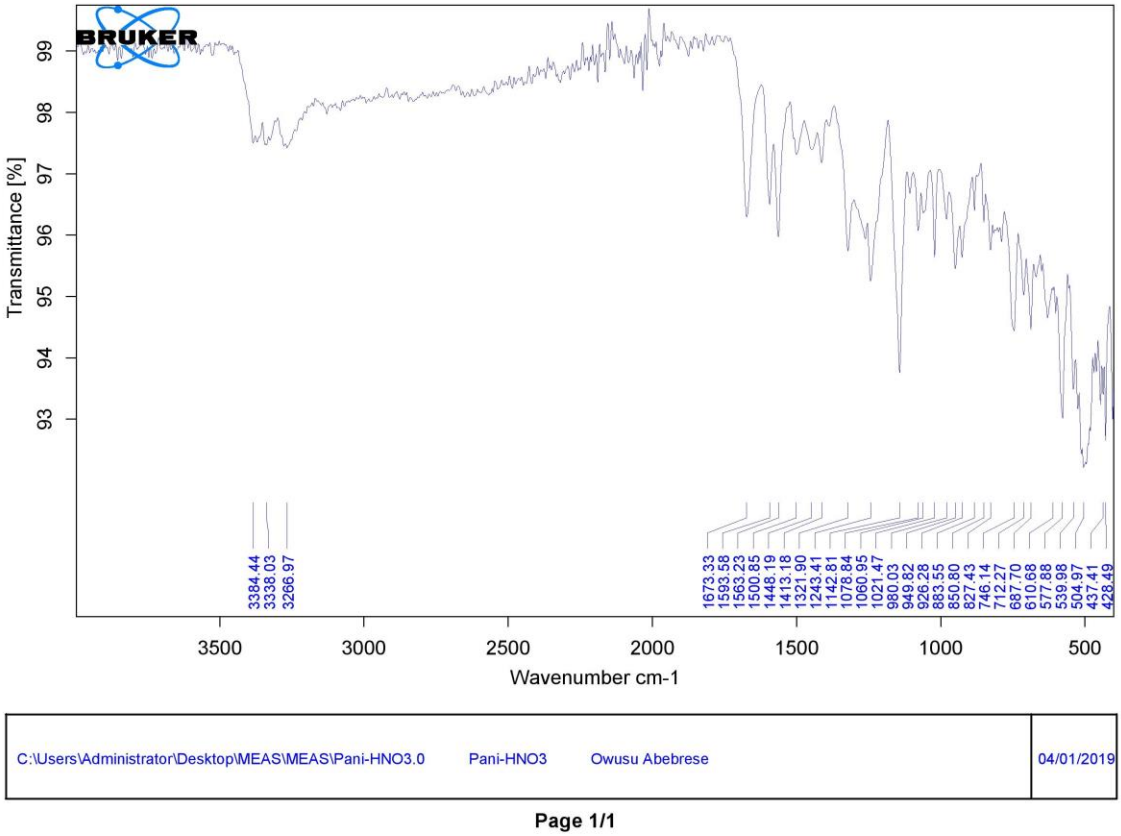


stretching appears at a much higher wavenumber that is at 1561 $cm^{-1}$ for PANI-HCl and 1561 $cm^{-1}$ for PANI-$H_2SO_4$

Figure 4.2: FTIR of PANI-$HNO_3$ thin film

The band at 1481 $cm^{-1}$ in both the PANI-HCl and PANI-$CH_3COOH$ can be attributed to the

benzenoid (B) ring stretching. That of PANI-$H_2SO_4$ occurs at 1478 $cm^{-1}$ whilst that of PANI-$HNO_3$ occurs at 1500 $cm^{-1}$. An absorption band in at 1300 $cm^{-1}$ and 1321 $cm^{-1}$ for samples PANI-$CH_3COOH$ and PANI-$HNO_3$ respectively corresponds to $\pi$-electron delocalization induced

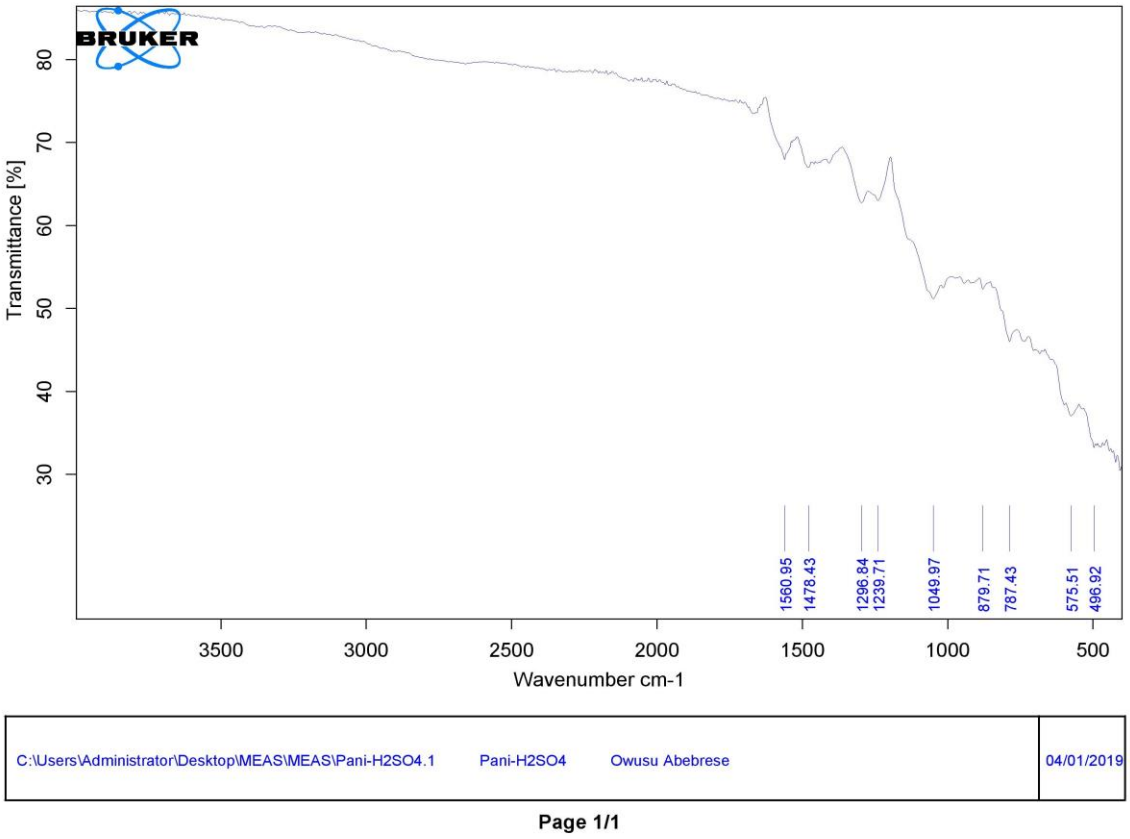


Figure 4.3: FTIR of PANI-$H_2SO_4$

in the polymer by protonation. The wavenumber at 1239 $cm^{-1}$ in both PANI-HCl and PANI-$CH_3COOH$ is characteristic of the conducting polymer.

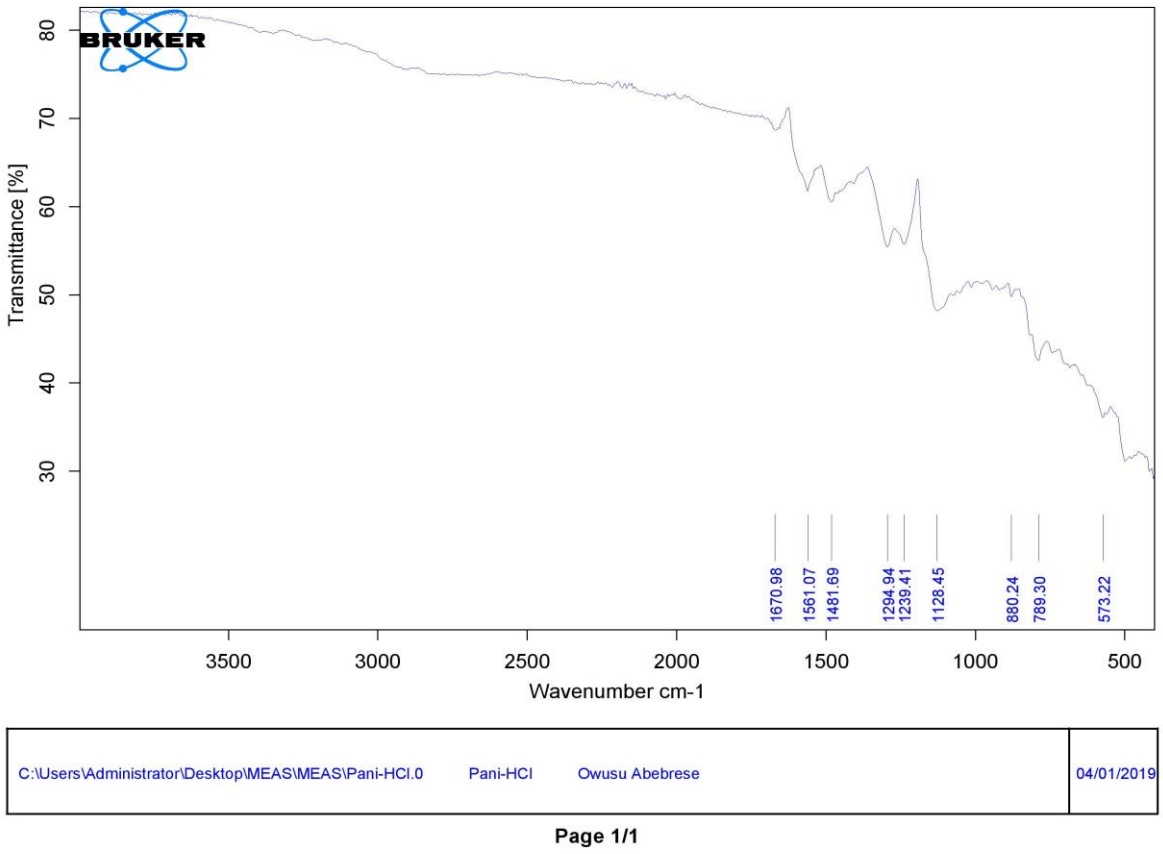


Figure 4.4: FTIR of PANI-HCl Thin Film

A band at the 1049 $cm^{-1}$ in the PANI-$H_2SO_4$ represents n S=O bonding for the camphor sulfuric acid. The band at 879 cm-1 in the PANI-$H_2SO_4$, which is a protonated sample, represents the $H_2SO_4$ – counterion.

At 827 820 for PANI-$HNO_3$ and $CH_3COOH$ respectively the bands present can be 1,4 – substituted benzene rings. For samples PANI-$H_2SO_4$ and PANI-HCl the quinoid bands are at 1561 $cm^{-1}$ for both samples and the benzenoid bands are at 1478 $cm^{-1}$ and 1481 $cm^{-1}$ respectively. The IQ/IB ratio as reported by (Melad et al., 2016) to give the degree of oxidation indicates that both samples had similar degree of oxidation. Also the band that confirms the presence of protonated imine function were found at 1563 $cm^{-1}$, 1560 $cm^{-1}$,1561 $cm^{-1}$ and 1553 $cm^{-1}$ for PANI-$HNO_3$, PANI-$H_2SO_4$, PANI-HCl and PANI-$CH_3COOH$ respectively. Furthermore the band at 1246 $cm^{-1}$ which according to (Atassi et al.,2008) is a characteristics of protonated form of PANI was found in the thin film samples at 1239 $cm^{-1}$, 1239 $cm^{-1}$, 1243 $cm^{-1}$ and 1208 $cm^{-1}$ for PANI-HCl, PANI-$H_2SO_4$, PANI-$HNO_3$ and PANI-$CH_3COOH$.

**FTIR of Bulk Samples**

Perkin Elmer Spectrum Version 10.08.09 was used to carry out the IR for the samples dried at 700 $^0$C. Below is the table for the absorption observed for each sample.

Table 4.1 Fourier Transformation Infrared Spectroscopy of the Bulk Samples

| SAMPLE | N-H stretching | C-H stretching | C = N stretching | Quinoid Bond | Benzenoid Bond | C-H out of plane |
|---|---|---|---|---|---|---|
| HCl | 3750 | 3053 | 1644 | 1596 | 1496 | 800 |
| $H_2SO_4$ | 3787 | - | 1650 | 1559 | 1473 | 800 |
| $HNO_3$ | 3787 | 3060 | 1647 | 1544 | 1437 | 824 |
| $CH_3COOH$ | - | - | - | 1559 | 1473 | 877 |

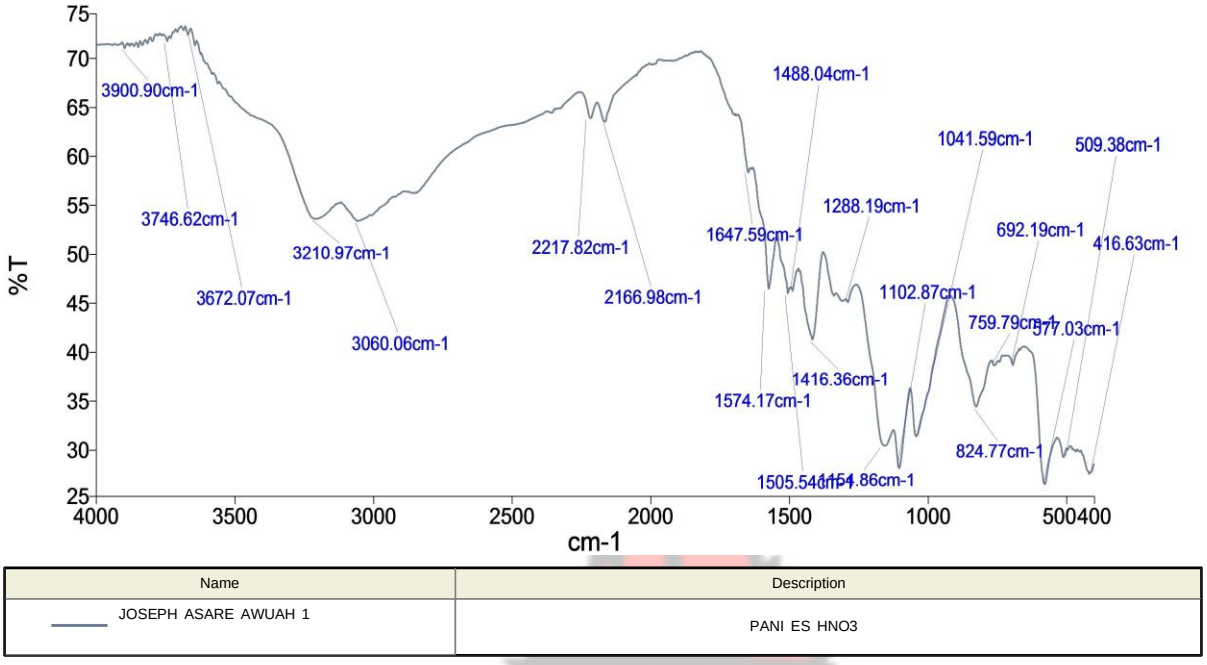


Figure 4.5: FTIR of PANI-$HNO_3$ Bulk sample

The Fig. 4.5 above shows the FTIR for the PANI-$HNO_3$ sample. The most significant bands for a protonated sample were observed in the bands at 1574.17 $cm^{-1}$ and 1488 $cm^{-1}$. The ring-stretching vibrations of the quinonoid and benzenoid rings of aniline can be attributed to the 1574.17 $cm^{-1}$ and 1488 $cm^{-1}$ bands respectively. The band at 3060 $cm^{-1}$ is due to the C-H stretching aromatics which is very strong. There was a weak C=N stretching band at the 2217.82 $cm^{-1}$. The mono substituted benzene is a clear characteristic observed in the absorption peak at 1041.59 $cm^{-1}$. The band at 824.77 $cm^{-1}$ was attributed to the out of plane C-H bending.

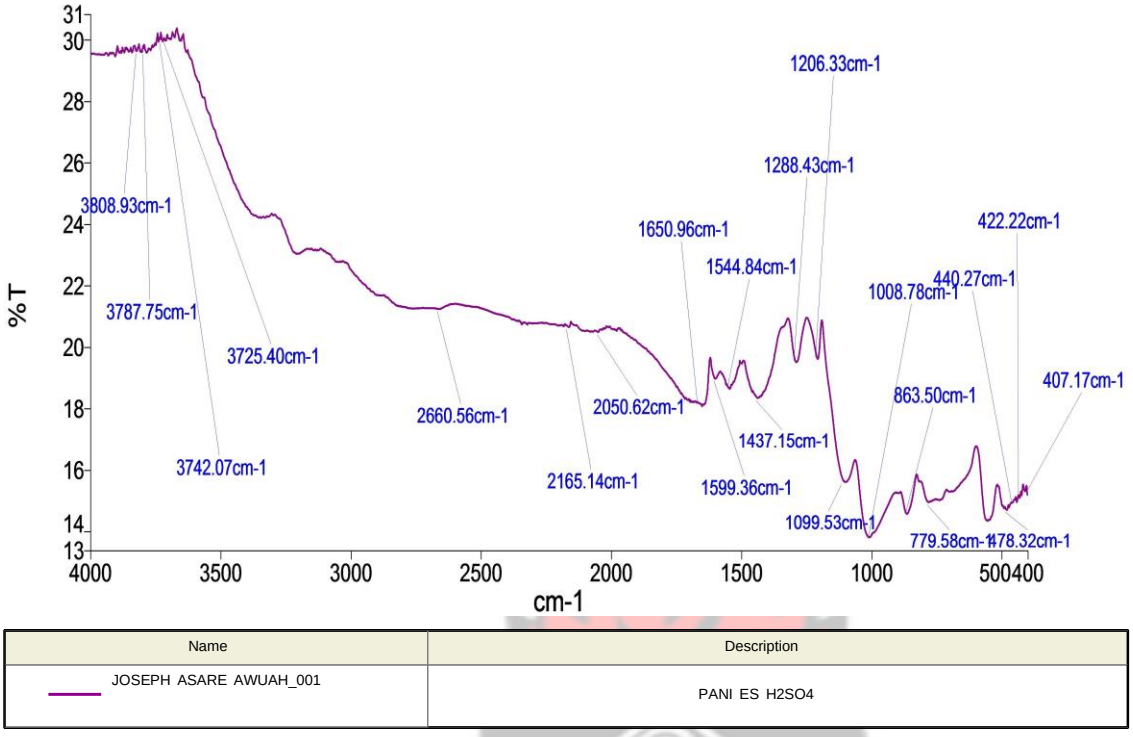


Figure 4.6: FTIR of PANI-$H_2SO_4$ Bulk sample

The bands at 3742.7 $cm^{-1}$ and 3787.75 $cm^{-1}$ are attributed to hydrogen-bonded N-H stretching. The wavenumbers 2660.56 $cm^{-1}$, 2165.14 $cm^{-1}$ and 2050.62 $cm^{-1}$ are due to absorption of free charge- carriers in the protonate polymer. The quinonoid and benzenoid ring-stretching vibrations were at the 1544.84. A blue shift can be observed for the quinonoid caused be the vibrations at the previous frequency to 1599.36 $cm^{-1}$ the band at 863.50 $cm^{-1}$ in the spectrum of the protonated sample represents the $H_2SO_4$ – counterion.

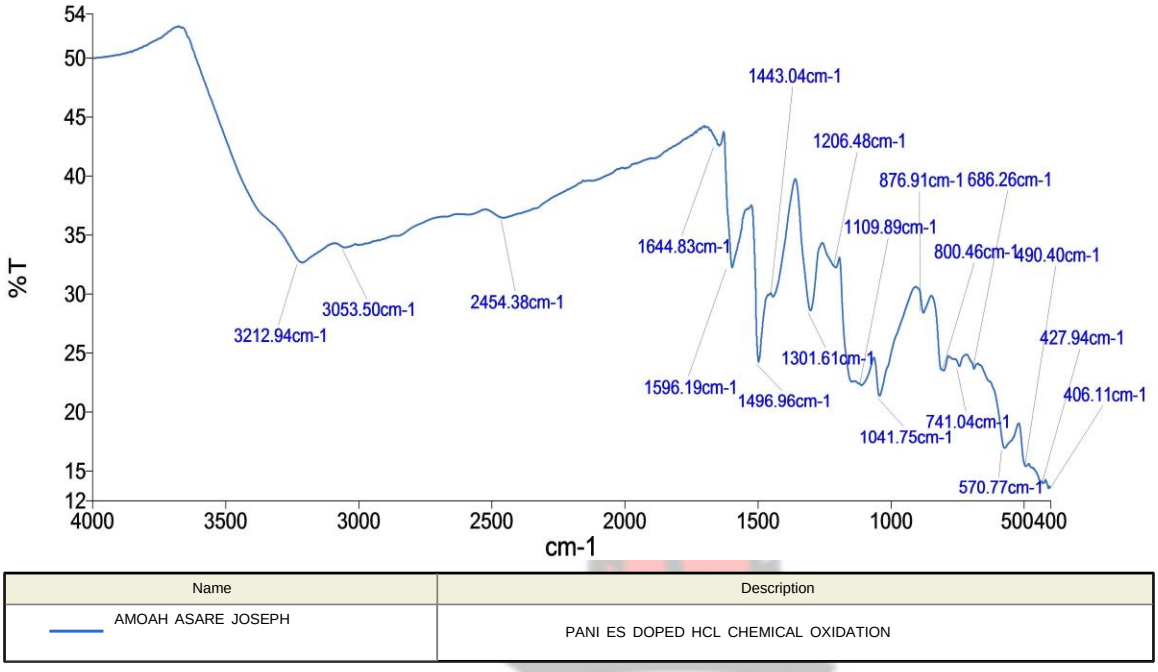


Figure 4.7: FTIR of PANI-HCl Bulk sample

The figure above shows the IR of PANI-HCl sample. The bands at 3212.94 $cm^{-1}$ and 3053.50 $cm^{-1}$ are attributed to hydrogen-bonded N-H stretching and the aromatic C-H stretching. The bands at 1596.19 $cm^{-1}$ and 1496 $cm^{-1}$ can be attributed to the quinonoid and benzoid structure of PANI $cm^{-1}$ in the spectrum of the sample corresponds to the $\pi$-electron delocalized induced in the polymer by protonation. The band observed at 1206.48 $cm^{-1}$ is a characteristic of the conducting protonated form of PANI.

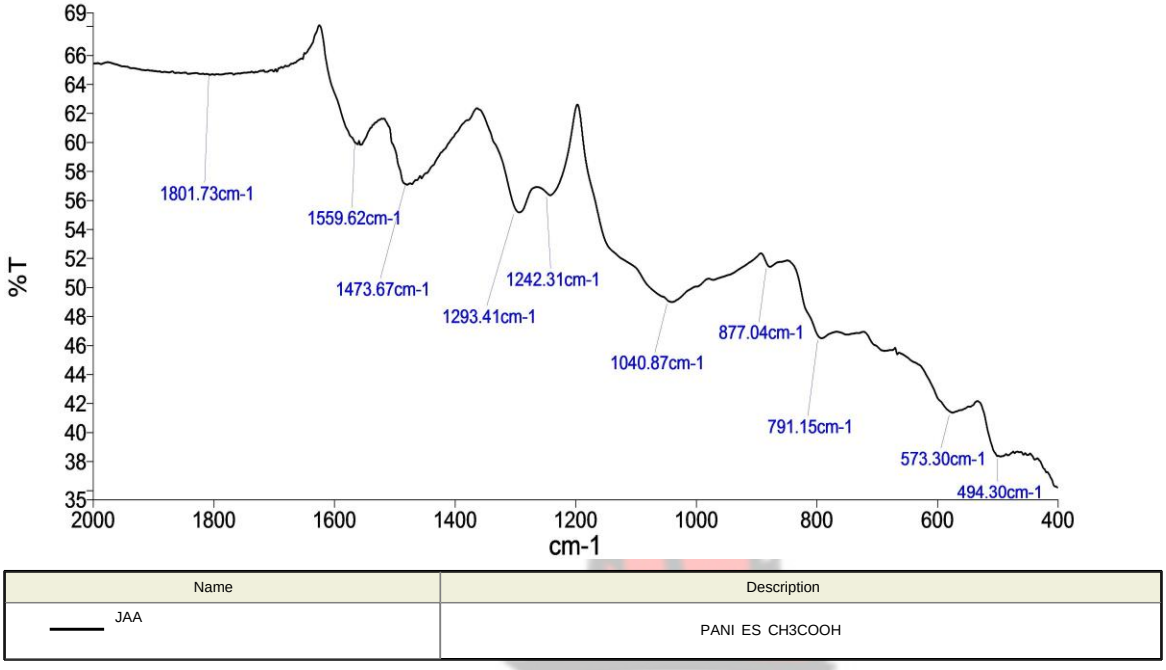


Figure 4.8: FTIR of PANI-$CH_3COOH$ Bulk sample

The quinoid and benzenoid ring-stretching were found at the 1559.62 $cm^{-1}$ and 1473.67 $cm^{-1}$ respectively. The band characteristic of conducting protonated form was observed at 1242.62 $cm^{-1}$. The 877.04 $cm^{-1}$ band can be attributed to the C-H out of plane bending vibrations of hydrogen atoms.

Bands at 1559 $cm^{-1}$ and 1473 $cm^{-1}$ are assigned to quinoid and benzenoid respectively for PANI-$CH_3COOH$. The same bands were observed for PANI-$H_2SO_4$ . The ratio of IQ/IB can be used to estimate the degree of oxidation state. The similarities observed in these two samples point to the fact that the oxidation degree in the two dopants is the same. The IQ/IB ratio for PANI-HCl and PANI-$HNO_3$ samples were not the same in comparison to any of the samples. This indicates that these samples had different degrees of oxidation (Melad et al.,2016). According to (Atassi et al.,2008) band characteristics of protonated form of PANI is observed at 1246 $cm^{-1}$ and this has been interpreted as originating from bi-polaron structures related to C-N stretchching vibration. In

this work bands at 1288 $cm^{-1}$,1206 $cm^{-1}$,1242 $cm^{-1}$ and 1206 $cm^{-1}$ were observed for PANI-$HNO_3$, PANI-$H_2SO_4$, PANI-$CH_3COOH$ and PANI-HCl respectively. Also peaks at 1580 $cm^{-1}$ have been reported to confirm the presence of a protonated imine function (Rao et al., 2000). PANI-$HNO_3$, PANI-$H_2SO_4$, PANI-$CH_3COOH$ and PANI-HCl the peaks recording around this band were 1574 $cm^{-1}$, 1544 $cm^{-1}$, 1559 $cm^{-1}$ and 1598 $cm^{-1}$ respectively.



### 4.2 UV-Vis OF BULK SAMPLES

The absorption bands observed are usually within the ranges of 290-324, 402-430 and 828-835nm for a pure PANI (Owusu-Sekyere et al., 2017). The figure below shows a block diagram of optical detection systems of bulk samples of polyaniline using the various acids employed in this experiment. There are some bands that are characteristics of polyaniline.

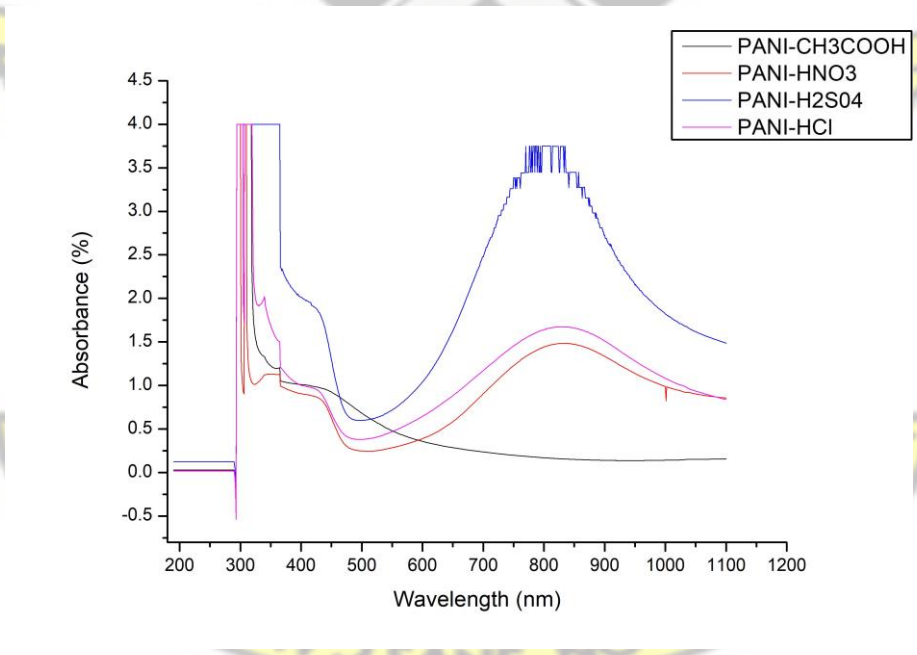


Figure 4.9: Absorbance versus wavelength of Bulk samples

The bands observed in all the four samples are in the stated ranges according to literature. For the weak acids PANI–$CH_3$*COOH*, the bands observed are in the range of 350-365, 430-440 and 770-

800 nm. The polaron and bipolaron bands which are clear characteristics of PANI can be seen in the range for the acetic acid. Similarly, the bands in PANI-$HNO_3$ appears in the ranges of 335-360 nm which is attributed to the $\pi$ - $\pi$* electron transition, polaron is observed in the 410-440 nm band and 700-800 nm been the band for transition between benzenoid-quinoid rings. Among the two weak acids it was observed that for $HNO_3$ the bands stretched further as compared to that of the acetic acid.



The bands that appear in the PANI-HCl sample were 310-400 nm, 420- 440 nm which show the presence of polarons and bipolarons transitions and the 700-810 nm band which can be attributed to charge transfers from the benzenoid and quinoid rings. In the same way these bands appeared in the PANI-$H_2SO_4$ sample. The absorption bands that have been obtained from the UV-Visible spectra are in good agreement with that reported in the literature.

Although the samples synthesized using different aqueous acids did show the various bands characteristic of PANI. Some comparisons can be made in terms of the bands and how they appeared via the spectral lines for each sample. To begin with are PANI$CH_3COOH$ and PANI-$HNO_3$. Although the transition in both occurs within the same band the difference in the wavelength could possibly be as results of the electron making a bigger jump from the pi bonding to pi anti-bonding state in PANI-$HNO_3$. This scenario runs throughout the entire bands when comparing PANI-$HNO_3$ to PANI-$CH_3COOH$.

The transition of the pi bonding to the pi anti-bonding in PANI-$H_2SO_4$ occurs earlier than in PANI-HCl sample. This can only be as a results of the $H_2SO_4$ acid been a stronger acid than the HCl and as a results the transition from $\pi$ - $\pi$* required lower wavelength for PANI-$H_2SO_4$ sample as compared to the PANI-HCl sample. By comparing the four samples the $\pi$ - $\pi$* transition then can be arranged from the strongest to the weakest as PANI-$H_2SO_4$ followed by PANI-HCl then PANI-$HNO_3$ and the weakest been PANI-$CH_3COOH$.



### 4.2.1 Determination of the Band Gap of Bulk Samples

Using the Stern relation below (Stern, 1963), the energy band gaps (Eg) of the thin films were established by the absorbance spectra.

$$A = \frac{K(hv - Eg)^{\frac{n}{2}}}{hv} \quad (4.1)$$

Where *hv* is the photon energy, A is the absorbance; K equals a constant while *n* carries the value of either 1 or 4. In a direct transition n is equal to 1 and 4 for allowed and forbidden transitions respectively. The band gap, Eg, were obtained from a straight line plot of $(Ahv)^2$ as a function of *hv*. Extrapolation of the line to intersect the horizontal axis at $(Ahv)^2 = 0$, gave the energy band gap as shown in the figures below. The Eg obtained were 3.30 eV, 3.75 eV, 3.83 eV and 3.89 eV for PANI-HCl, PANI-$H_2SO_4$, PANI-$HNO_3$ and PANI-$CH_3COOH$ respectively.

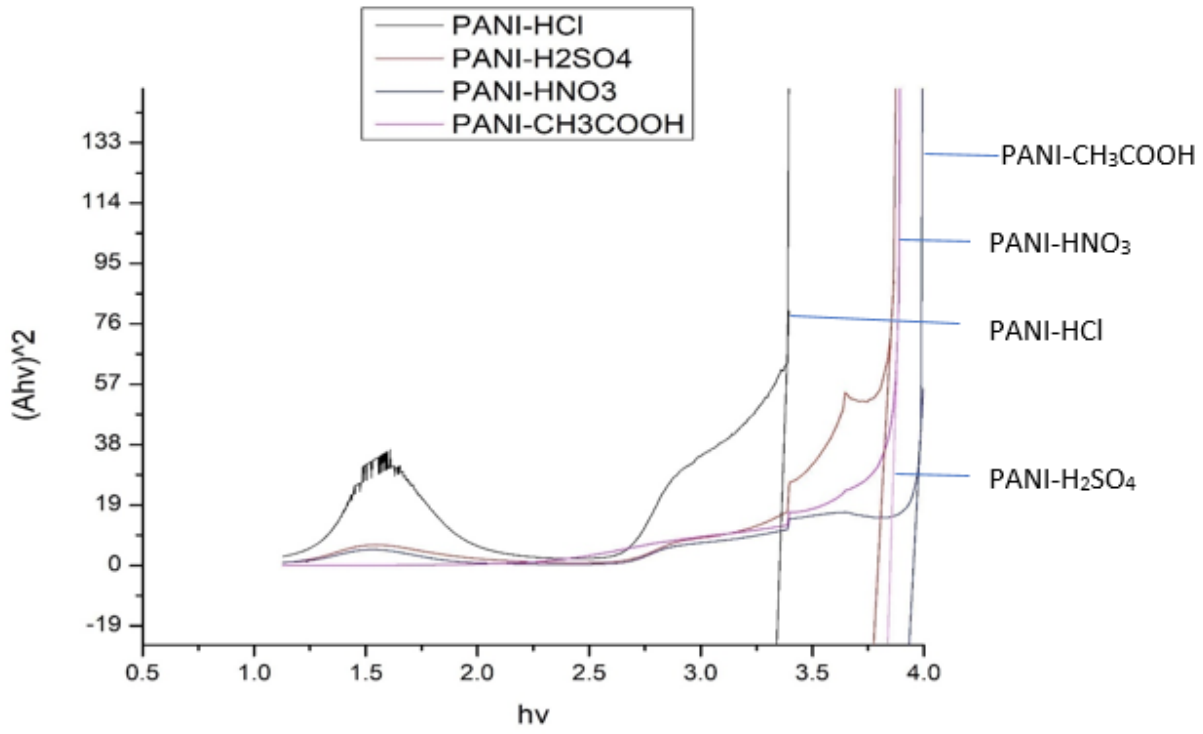


Figure 4.10: Band Gap of Bulk samples

### 4.3 UV-Vis OF THIN FILM SAMPLES

The absorption observed for the thin films occurs between the ranges of 320-375, 400-480 and 600-720 nm. These wavelengths reveal the electron transition in the thin film samples. Just as in the bulk samples there is first the $\pi$ - $\pi$* electron transition which occurs earliest in the weak acids between the wavelength 320-375 nm and then the polaron (transitions) typical of polyaniline occuring within the range of 400-480 nm. The electron transition between the benzenoid and quinoid rings occurs at 600-720 nm. The transitions occurring in the polaron, benzenoid and quinoid of the thin film occurs in all the samples. The clear difference is in the $\pi$ - $\pi$* transition which for the PANI-HCl and PANI-$H_2SO_4$ occurred at a much higher wavelength.

In both the thin films and bulk samples there was no shift from <300 nm to >300 nm. According to (Melad et al.,2016) such shifts are due to the steric effect which hinders charge transfer between chains and leads to low conductivity in the material.

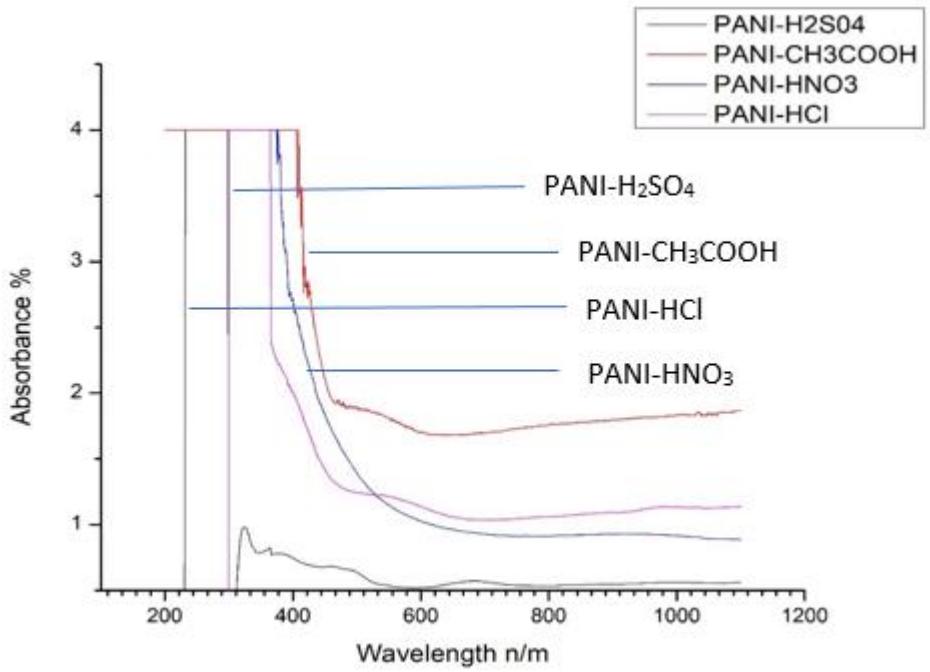


Figure 4.11: Absorbance versus wavelength of Thin Film samples

### 4.3.1 Determination the Band Gap of Thin Film Samples

The Eg obtained were 3.00 eV, 2.60 eV, 3.36 eV and 4.1 eV for PANI-HCl, PANI-$H_2SO_4$, PANI-$HNO_3$ and PANI-$CH_3$*COOH* respectively.

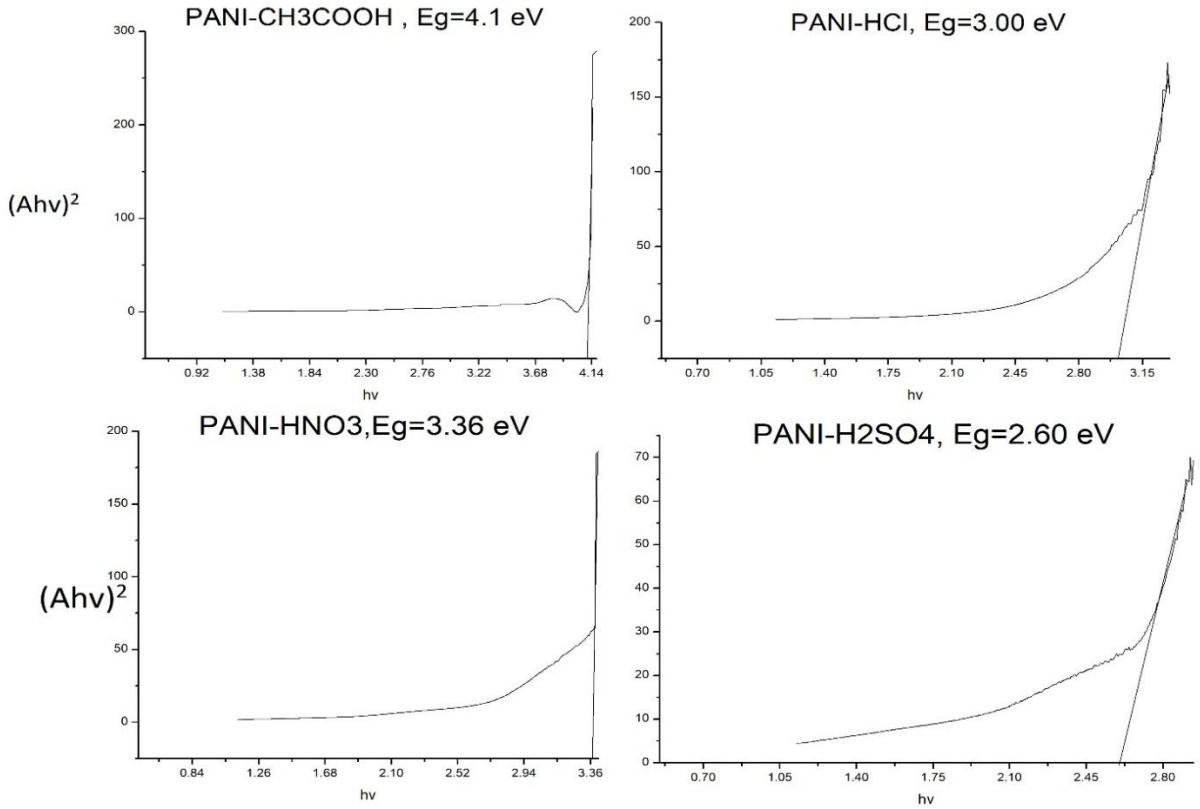


**Figure** 4.12: Band Gap of Thin film samples

Table 4.2 Band gap of Thin film and Bulk samples.

| SAMPLE | Thin film (Eg/eV) | Bulk sample (Eg/eV) |
|---|---|---|
| HCl | 3.00 | 3.30 |
| $H_2SO_4$ | 2.60 | 3.75 |
| $HNO_3$ | 3.36 | 3.83 |
| $CH_3COOH$ | 4.10 | 3.89 |

The band gap is in agreement to the conductivity of the PANI samples

## 4.4 CYCLIC VOLTAMMOGRAMS OF THIN FILMS

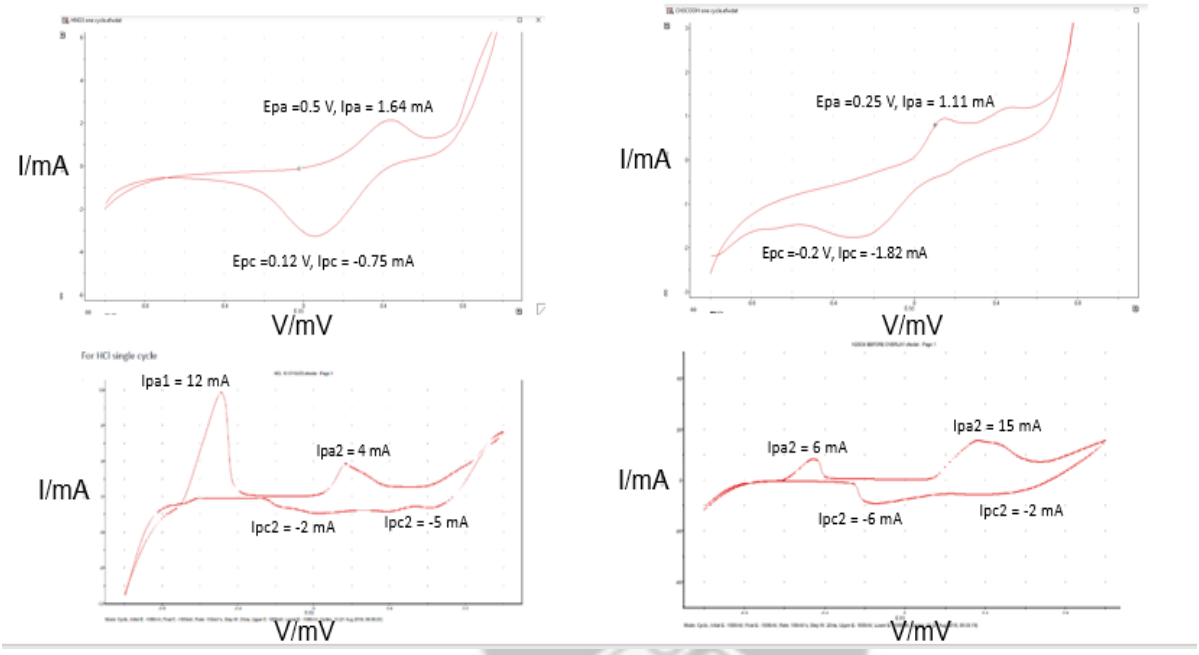


**Figure** 4.13: Voltamographs Thin film samples

Cyclic voltammetry was used to study the qualitative information about the electrochemical process in synthesizing PANI by electrodeposition on an ITO glass with aqueous acids forming part of the electrolyte. Cyclic voltammograms obtained from the electrochemical process using the eDaQ software integrated into the POTENTIOSTAT 468 device. The electrochemical behavior of polyaniline is dependent on the applied potential and the surface area of the electrodes (Song et al., 2013). The cyclic voltammograph (CV) show two set of distinct redox reaction. That is two pairs of anodic and cathodic current peaks with potential peaks also. This was observed in the voltammograph for HCl and $CH_3COOH$. A single current peak and potential peak are observed for both cathodic and anodic processes from the voltammograph. The CV curve for $CH_3COOH$ shows a set of redox couple between the potential E= -0.29 V and +0.134 V using the Ag/AgCl as reference electrode. This is related to the conversion of fully reduced leucoemeraldine base to the

partially oxidized emeraldine. The second set of redox couple occurs between the potentials E = +0.63 V and E = -0.25 V using Ag/AgCl can be related to the conversion of emeraldine to the fully oxidized pernigraniline.

For all the four samples it was observed that the oxidation peak and its corresponding reduction peak appeared to move to more negative values at the scan rate used which was 100 mV/s. This implies that the protons are involved in the reaction unlike the first peaks. The anodic peak observed at more positive potentials of E = +0.13 – 0.73 V for CH3*COOH*, E =+0.22 – 0.74 V for $H_2SO_4$ , E = +0.20 – 0.83 V for HCl and E = +0.41 – 0.77 V for $HNO_3$ was very strong in the first cycle of the anodic branch for the case of each electrolyte used in the experiment. This can be attributed to the initial monomer oxidation according to (Genies et al., 1987).

Almost all the monomer were oxidized between the potentials of E = +0.73 to +0.83 V/S.C.E and afterwards a redox equilibrium was installed at E = -0.20 v for $CH_3$*COOH*, $H_2$SO4 and HCl except $HNO_3$ which was installed at a potential of E = +0.06 V. The voltammograph show a narrow anodic-cathodic peak of the polymer and according to (Genies and Lapkowski, 1987) that shows the polyaniline synthesized is highly conductive (Bejan et al., 1998) revealed that for a Pt as counter electrode, reduction will always prevail and that was experienced in all the four electrolytes used in this experiment.

## 4.5 CONDUCTIVITY OF SAMPLES

Using the four point probe requires the use of the equation below:

$$\rho = 4.5324t\frac{V}{I} \tag{4.12}$$

Where; $\rho$ = resistivity of the material, the reciprocal which gives the DC conductivity, σ,

since $\sigma = 1/\rho$

I = Average current supplied to the entire set-up

V = Average voltage drop measured across the sample

t = thickness of the sample

For the bulk samples a micrometer screw-gauge was used to measure the thickness. Equation below was used:

$$t = \frac{m}{\rho A} \tag{4.13}$$

Where: $\rho$ in this equation represents the density of PANI

m = mass of the sample obtained by subtracting the mass of the ITO from the mass of the ITO with the sample after deposition.

A = Area of the sample obtained by multiplying the length x width, ($l$ x w) of the sample.

Below is the data obtained for calculating the resistivity of the thin film and bulk samples.

Density of PANI is given by 1.326 ± 0.014 g/mL (Stejskal., 2011 )

The mass of the substrate, ITO 1.215 g

Table 4.3 Data for determining the thickness of the Thin film sample

| DOPANT | Length l/cm | Breath b/cm | Initial Mass m/g | Final Mass m/g |
|---|---|---|---|---|
| HCl | 3.00 | 1.20 | 1.45 | 0.24 |
| $H_2SO_4$ | 2.80 | 1.20 | 1.39 | 0.17 |
| $HNO_3$ | 3.10 | 1.20 | 1.47 | 0.25 |
| $CH_3COOH$ | 3.00 | 1.20 | 1.37 | 0.15 |

Table 4.4 Thickness of Thin film and Bulk samples

| DOPANT | THICKNESS OF THIN FILM t/ $10^3$ μm | THICKNESS OF BULK SAMPLE t/$10^3$ μm |
|---|---|---|
| HCl | 0.048 | 0.322 |
| $H_2SO_4$ | 0.038 | 0.438 |
| $HNO_3$ | 0.051 | 0.367 |
| $CH_3COOH$ | 0.031 | 0.371 |

Table 4.5 Resistivity and Conductivity of Thin Film Samples

| DOPANT | AVERAGE CURRENT I/mA | AVERAGE VOLTAGE V/mV | ρ / Ω.cm | σ/ $S.cm^{-1}$ | σ/ $S.cm^{-1}$ from literature | Reference |
|---|---|---|---|---|---|---|
| HCl | 2.00 | 3.10 | 0.337 | 2.967 | 1.79 | (Owusu-Sekyere et al., 2017) |
| $H_2SO_4$ | 2.00 | 3.40 | 0.292 | 3.424 | 1.23 | (Vivekanadan et al., 2011). |
| $HNO_3$ | 2.00 | 8.60 | 0.994 | 1.006 | | |
| $CH_3COOH$ | 2.00 | 14.20 | 0.998 | 1.002 | | |

Table 4.6 Resistivity and Conductivity of Bulk Samples.

| DOPANT | AVERAGE CURRENT I/mA | AVERAGE VOLTAGE V/mV | ρ / Ω.cm | σ/ S.cm$^{-1}$ | σ/ S.cm$^{-1}$ from literature | Reference |
|---|---|---|---|---|---|---|
| HCl | 1.95 | 2.00 | 1.956 | 0.669 | 0.16 | (Sinha et al., 2016) |
| $H_2SO_4$ | 2.35 | 1.00 | 0.578 | 1.183 | 1.09 | (Alesary et al., 2018) |
| $HNO_3$ | 0.35 | 0.70 | 2.719 | 0.300 | 0.04 | (Manaf et al., 2016) |
| $CH_3COOH$ | 0.25 | 1.00 | 5.438 | 0.148 | 0.04 | (Kulkarni et al., 2004). |

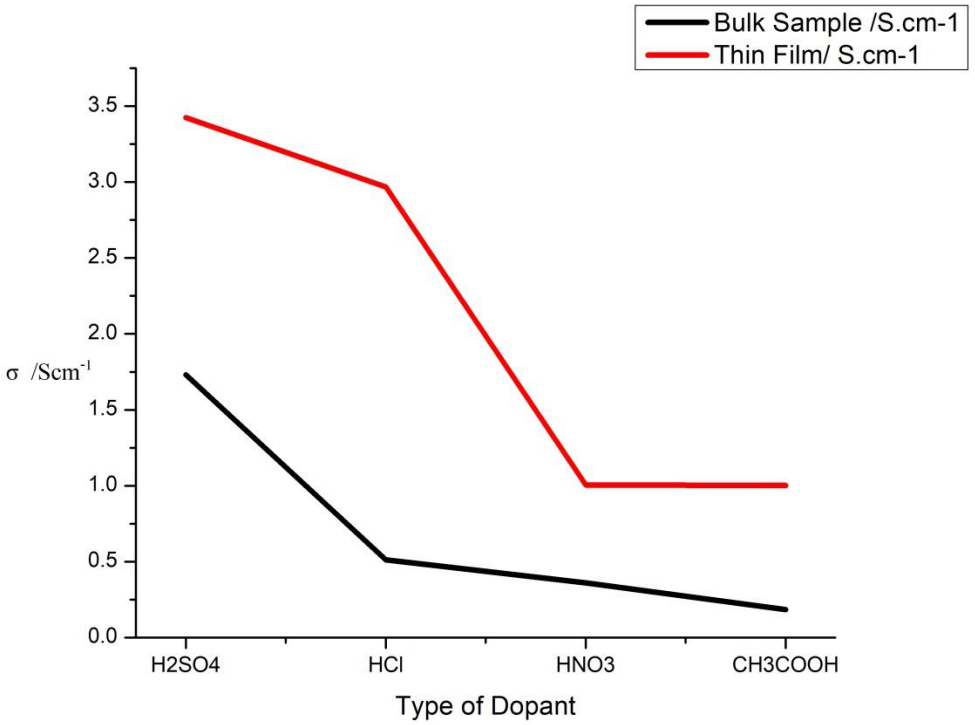


Figure 4.14 Graph of Conductivity against Type of Dopant for Thin films and Bulk samples.

The conductivity values for PANI-HCl, PANI-$H_2SO_4$ and PANI-$HNO_3$ are seen to be greater than the organic acid and the same trend is observed in all the samples. According to (Heinze et al., 2010) dopants possessing sulfonate counter ion are capable of forming hydrogen bonds resulting in enhanced DC conductivity and that is why PANI-$H_2SO_4$ had the greatest conductivity than the others. Another reason is that proton dissociation from the acid is of importance due to its effect on the protonation (Kim et al, 2014) and $H_2SO_4$ has the highest acid dissociation constant followed by HCl and $HNO_3$.

The conductivity value for PANI-HCl in this work was 6.69 x $10^{-1}$ S/cm which is greater than the reported 1.6 x $10^{-1}$ (Sinha et al., 2016). In their work the reaction medium were kept at 0$^{o}$C which could be the reason for low conductivity for the chemically synthesised PANI-HCl. All reactions in this work were performed at room temperature. According to (Priyanka et al. 2015) at high temperatures conductivity increases due to the hopping of polarons from one localised state to another localised state. Another factor that might have contributed to the differences although the concentration of the dopants is the same would be the volume of the dopant used.

Alesary reported a conductivity value of 1.09 S/cm for polyaniline doped with $H_2SO_4$ (Alesary et al., 2018). In this work the conductivity of PANI- $H_2SO_4$ by chemical oxidation method was 1.183 S/cm which was not so far from the literature. Although 1 M of $H_2SO_4$ was used in both cases the difference in volume of the dopant in the APS solution and aniline solution could be the reason for the difference in conductivity. One other factor is the temperature at which polymerization was allowed to occur. In this work all the synthesis was done at room temperature whilst Alesary conducted his work at a lower temperature (0-1) $^{o}$C.

(Manaf et al., 2016) reported that the value of conductivity at 0.04 S/cm when polyaniline was doped with $HNO_3$ indicated that the anionic of nitric ($NO_3^-$) was not able to increase the conductivity level of PANI-ES. This was observed in this work, the value of PANI-$HNO_3$ was the lowest in comparison with the inorganic acids used in the experiment. Kulkani also reports of the low conductivity in the organic dopant synthesised by chemical oxidation at (0-5) $^oC$ to be 4.21 x $10^{-2}$ S/cm, in this work the conductivity of PANI-$CH_3COOH$ was recorded as 1.48 x $10^{-1}$ S/cm which was lower than the other dopants but higher in comparison with the previous study (Kulkarni et al., 2004).

The conductivity pattern for the electrochemically synthesised samples is in agreement with the report given by (Mamman et al. 2013). In their work, they reported that the dopant $H_2SO_4$ had the highest conductivity than HCl doped polyaniline and similar observation was made in this work. The conductivity of PANI-HCl in Owusu-Sekeyere work was 1.79 S/cm, in this work PANI-HCl thin film had a conductivity of 2.96 which is am improvement of the previous study. The difference in the results can be attributed to the pH of the electrolyte used during the deposition. In his work he reported that a low pH has more charge carriers. Vivekanadan also reported in their work on the conductivity of PANI- $H_2SO_4$ synthesised by both chemical and electrochemical methods at room temperature. In his report the bulk sample had a conductivity value of 0.27 S/cm whilst the highest conductivity recorded for the thing film was 1.23 S/cm (Vivekanadan et al., 2011). Similar trend was observed in this wok, for the bulk sample, the PANI- $H_2SO_4$ had a conductivity of was 1.183 S/cm whilst that of the thin film was 3.424 S/cm. This can be attributed to the regular arrangement of the monomer units in the thin film than that of the PANI- $H_2SO_4$ bulk sample.

# CHAPTER 5

## CONCLUSION AND RECOMMENDATION



### 5.1 CONCLUSION

Polyaniline, PANI-ES was synthesized using four different dopants (HCl, $H_2SO_4$, $HNO_3$ and $CH_3COOH$) and the methods used were chemical oxidation and electrochemical oxidation. Absorption peak was observed between the ranges of 300-350 nm which depicts the $\pi - \pi^*$ electron transition. Another peak between 450 – 540 nm was also noticed for in all the samples and can be attributed to the polaron and bipolaron transition in polyaniline. This observation was made in all the samples prepared by the different methods. The optical band gap determined using the Sterns relation was between the 3.20 – 3.95 eV for the bulk samples. The band gap for the thin film samples were determined to be in the range of 2.60-3.83 eV. Better conductivity of 3.424 S/cm for thin film and 1.183 S/cm for bulk sample were observed for the polyaniline doped with $H_2SO_4$ and it can be ascribed to the electron transfer in the structure as obtained form the UV-Vis analysis. HCl and $HNO_3$ acid doped samples resulted in moderate conductivity while $CH_3COOH$ doped samples had the least conductivity which was due to the decrease in localised defect states in the polaron bond indicate by the low intense bond observed from the UV-Vis. The main strength of thin film technology is in micro-electronics through large scale integrated circuits. This work gives further proof and confirmation of the strength and power of micro-electronics, now and deep into the future with conducting polymers. The result from this work gives the evidence

for the future development of micro-electronics with conducting polymers. Also, the results show that, the band gaps of the thin film samples were much lower than those of the bulk samples. The results of the work satisfy one key requirement for successful electronic device design and development, which is high conductivity.



## S5.2 RECOMMENDATION

1. 1. Polyaniline (PANI) composites using the different dopants should be synthesized to produce thin films of high reflectivity to be used manufacturing opto-electronic application and also to be used for LED.

2. X-ray diffraction should be performed for structural analysis to see the effect of various elements constituting the composites.

## REFERENCES


M. Akay. *Introduction to Polymer Science and Technology*. Bookboon, 2012.

R. G. Bavane. Synthesis and characterization of thin films of conducting polymers for gas sensing applications. 2014.

D. Bejan and A. Duca. Voltammetry of aniline with different electrodes and electrolytes. *Croaticachemica acta*, 71(3):745–756, 1998.

S. Bhadra, N. K. Singha, and D. Khastgir. Electrochemical synthesis of polyaniline and its comparison with chemically synthesized polyaniline. *Journal of applied polymer science*, 104(3):1900–1904, 2007.

Z. A. Boeva and V. G. Sergeyev. Polyaniline: Synthesis, properties, and application. *Polymer Science Sseries C*, 56(1):144–153, 2014.

B. A. Bolto, R. McNeill, and D. Weiss. Electronic conduction in polymers. iii. electronic properties of polypyrrole. *Australian Journal of Chemistry*, 16(6):1090–1103, 1963.

Y. Cao, P. Smith, and A. J. Heeger. Counter-ion induced processibility of conducting polyaniline and of conducting polyblends of polyaniline in bulk polymers. *Synthetic Metals*, 48(1):91–97, 1992.

A. J. Chavan. Use of plastic waste in flexible pavements. *International Jjournal of Application or Innovation in Engineering and Management*, 2(4): 540–552, 2013.

Atassi, Yomen and Tally, Mohammad and Ismail, Mazen, Synthesis and characterization of chloride doped polyaniline by bulk oxidative chemical polymerization. Doping effect on electrical conductivity, arXiv preprint arXiv: 0809.3552, 2008.

Alesary, Hasan Fisal and Ismail, Hani Khalil and Khudhair, Ahmed Fadhil and Mohammed, Mohammed Qasim, Effects of dopant ions on the properties of polyaniline conducting polymer, Oriental Scientific Publishing Company, 2525, 2018

Y.-J. Cheng, S.-H. Yang, and C.-S. Hsu. Synthesis of conjugated polymers for organic solar cell applications. *Chemical reviews*, 109(11):5868–5923, 2009.

G. Ciri´ c-Marjanovi´ c, M. Trchov´ a, and J. Stejskal.´ The chemical oxidative polymerization of aniline in water: Raman spectroscopy. *Journal of Raman Spectroscopy: An International Journal for Original Work in all Aspects of Raman Spectroscopy, Including Higher Order Processes, and also Brillouin and Rayleigh Scattering*, 39(10):1375–1387, 2008.

J. Daintith and E. A. Martin. *A dictionary of science*. Oxford University Press, USA, 2010.

A. Dallolio, G. Dascola, V. Varacca, and V. Bocchi. Electronic paramagnetic resonance and conductivity of a black electrolytic oxypyrrole. *ComptesRendusHebdomadaires Des Seances De L Academie Des Sciences Serie C*, 267(6):433, 1968.

R. De Surville, M. Jozefowicz, L. Yu, J. Pepichon, and R. Buvet. Electrochemical chains using protolytic organic semiconductors. *Electrochimica Acta*, 13(6):1451–1458, 1968.

D. DeLongchamp and P. T. Hammond.Layer-by-layer assembly of pe-

dot/polyaniline electrochromic devices. *Advanced Materials*, 13(19):1455–1459, 2001.

A. Diaz and J. Logan. Electroactive polyaniline films. *Journal of Electroanalytical Chemistry and Interfacial Electrochemistry*, 111(1):111–114, 1980.

L. A. Dissado and J. C. Fothergill. *Electrical degradation and breakdown in polymers*, volume 9. IET, 1992.

R. O. Ebewele. *Polymer science and technology*. CRC press, 2000.

P. J. Flory. *Principles of polymer chemistry*. Cornell University Press, 1953.

W. W. Focke, G. E. Wnek, and Y. Wei. Influence of oxidation state, ph, and counterion on the conductivity of polyaniline. *Journal of Physical Chemistry*, 91(22):5813–5818, 1987.

E. Genies and M. Lapkowski. Spectroelectrochemical evidence for an intermediate in the electropolymerization of aniline. *Journal of electroanalytical chemistry and interfacial electrochemistry*, 236(1-2):189–197, 1987.

J. F. Gordon. *The development of the designer children's wear industry, 19201969*. Iowa State University, 2016.

V. R. Gowariker, N. Viswanathan, and J. Sreedhar. *Polymer science*. New Age International, 1986.

G. W. Gribble. Pyrroles and their benzo derivatives: applications. *Comprehensive heterocyclic chemistry II*, 2:207–257, 1996.

A. J. Heeger. Semiconducting and metallic polymers: the fourth generation of polymeric materials (nobel lecture). *AngewandteChemie International Edition*, 40(14):2591–2611, 2001.

T. P. Henning, H. S. White, and A. J. Bard. Polymer films on electrodes. 6. bioconductive polymers produced by incorporation of tetrathiafulvalenium in a polyelectrolyte (nafion) matrix. *Journal of the American Chemical Society*, 103(13):3937–3938, 1981.

G. Inzelt. Historical background (or: There is nothing new under the sun). *Conducting Polymers: A New Era in Electrochemistry*, pages 265–269, 2008.

G. Inzelt. Historical background (or: There is nothing new under the sun). In *Conducting Polymers*, pages 295–297. Springer, 2012.

A. Jenkins, P. Kratochvil, R. Stepto, and U. Suter. Glossary of basic terms in polymer science (iupac recommendations 1996). *Pure and applied chemistry*, 68(12):2287–2311, 1996.

T. Kahl, K.-W. Schroder, F. Lawrence, W. Marshall, H. H¨ oke, and R. J¨ ackh.¨ Aniline. *Ullmann's Encyclopedia of Industrial Chemistry*, 2000.

E. Kang, K. Neoh, and K. Tan. Polyaniline: a polymer with many interesting intrinsic redox states. *Progress in polymer science*, 23(2):277–324, 1998.

H. Kasai, H. S. Nalwa, S. Okada, H. Oikawa, and H. Nakanishi. Fabrication and spectroscopic characterization of organic nanocrystals. In *Handbook of Nanostructured Materials and Nanotechnology*, pages 433–473. Elsevier, 2000.

G. B. Kauffman. Rayon: the first semi-synthetic fibre product. *Journal of chemical education*, 70(11):887, 1993.

T.-H. Le, Y. Kim, and H. Yoon. Electrical and electrochemical properties of conducting polymers. *Polymers*, 9(4):150, 2017.

H. Letheby. Xxix.—on the production of a blue substance by the electrolysisof sulphate of aniline. *Journal of the Chemical Society*, 15:161–163, 1862.

Y. Li. *Conducting Polymers*, page 23–50. Springer International Publishing, Cham, 2015.

D. Lin-Vien, N. B. Colthup, W. G. Fateley, and J. G. Grasselli. *The handbook of infrared and Raman characteristic frequencies of organic molecules*. Elsevier, 1991.

A. MacDiarmid and J. Chiang. Polyaniline': protonic acid doping of the emeraldine form to the metallic regime. *Synth. Met*, 13:193–205, 1986.

A. MacDiarmid, J. Chiang, A. Richter, Epstein, and AJ. Polyaniline: a new concept in conducting polymers. *Synthetic Metals*, 18(1-3):285–290, 1987.

A. G. MacDiarmid. "synthetic metals": A novel role for organic polymers

(nobel lecture). *AngewandteChemie International Edition*, 40(14):2581– 2590, 2001.

Z. Q. Mamiyev and N. O. Balayeva. Preparation and optical studies of pbs nanoparticles. *Optical Materials*, 46:522–525, 2015.

Kulkarni, Milind V and Viswanath, Annamraju Kasi and Marimuthu, R and Seth, Tanay, Synthesis and characterization of polyaniline doped with organic acids, Journal of Polymer Science Part A: Polymer Chemistry, Wiley Online Library, pages 2043—2049, 2004s.

L. K. Massey. *Permeability properties of plastics and elastomers: a guide to packaging and barrier materials*. William Andrew, 2003.

J. Masters, Y. Sun, A. MacDiarmid, and A. Epstein. Polyaniline: allowed oxidation states. *Synthetic Metals*, 41(1-2):715–718, 1991.

J. Moalli. *Plastics Failure Analysis and Prevention*. William Andrew, 2001.

K. M. Molapo, P. M. Ndangili, R. F. Ajayi, G. Mbambisa, S. M. Mailu,N. Njomo, M. Masikini, P. Baker, and E. I. Iwuoha. Electronics of conjugated polymers (i): polyaniline. *International Journal of Electrochemical Science*, 7(12):11859–11875, 2012.

Kofi Owusu-Sekyere, I. Nkrumah, R.K. Nkum, K.. Singh: Optical Behaviour of PANI/SNO2 Nano-Composite. *European Science Journal*. Volume 13, 2017).

H. Naarmann. Polymers, electrically conducting. *Ullmann's Encyclopedia of Industrial Chemistry*, 2000.

Heinze, Jurgen and Frontana-Uribe, Bernardo A and Ludwigs, Sabine, Electrochemistry of Conducting Polymers Persistent Models and New Concepts, Chemical Reviews, ACS Publications, 4724-4771, 2010.

T. Natarajah. Functional nanofibers in microelectronics applications. *Functional Nanofibers and their Applications*, page 371, 2012.

K. Neoh, E. Kang, and K. Tan. Evolution of polyaniline structure during synthesis. *Polymer*, 34(18):3921–3928, 1993.

Kim, Jongmin and Ju, Haeri and Inamdar, Akbar I and Jo, Yongcheol and Han, J and Kim, Hyungsang and Im, Hyunsik, Synthesis and enhanced electrochemical supercapacitor properties of Ag--MnO2--polyaniline nanocomposite electrodes, Elsevier, 473—477, 2014.

Melad, Omar and Jarur, Mariam , Studies on the effect of doping agent on the structure of polyaniline, Chemistry & Chemical Technology, Lviv Polytechnic National University, pages 41-44, 2016.

P. Nunziante and G. Pistoia. Factors affecting the growth of thick polyaniline films by the cyclic voltammetry technique. *Electrochimica acta*, 34(2):223– 228, 1989.

U. of Sydney. *http://www.materials.unsw.edu.au/tutorials/online-tutorials/1polymerisation*. 2013.

A. V. Pandya. Study of the comparison of conducting behavior of doped macromolecules and semiconductors. *Imperial Journal of Interdisciplinary Research*, 2(12), 2016.

J. K. Peter Atkins, Julio De Pala. *Physical Chemistry*, volume 11th Eedition.

Oxford University Press, 2017.

Z. Ping. In situ ftir–attenuated total reflection spectroscopic investigations on the base–acid transitions of polyaniline. base–acid transition in the emeraldine form of polyaniline. *Journal of the Chemical Society, Faraday Transactions*, 92(17):3063–3067, 1996.

J. Pople. The electronic spectra of aromatic molecules ii: A theoretical treatment of excited states of alternant hydrocarbon molecules based on selfconsistent molecular orbitals. *Proceedings of the Physical Society. Section A*, 68(2):81, 1955.

S. Poyraz. Synthesis and characterization of nanostructured conducting polymers and their composites with noble metal nanoparticles. 2010.

S. Pruneanu, E. Veress, I. Marian, and L. Oniciu. Characterization of polyaniline by cyclic voltammetry and uv-vis absorption spectroscopy. *Journal of materials science*, 34(11):2733–2739, 1999.

M. A. Rahman, P. Kumar, D.-S. Park, and Y.-B. Shim. Electrochemical sensors based on organic conjugated polymers. *Sensors*, 8(1):118–141, 2008.

Azwar Manaf, Yoga Julian Prasutiyo, Mas Ayuelitahafizah, Andreas, Synthesis And Effect Of Secondary Dopant On The Conductivity Of Conducting Polymer Polyaniline, Journal of Polymer Engineering, De Gruyter ,pages 785—792, 2013

Azwar Manaf, Yoga Julian Prasutiyo, Mas Ayuelitahafizah, Andreas, Synthesis and micowave characterization of conductive polyaniline prepared by continous polymerization process, IOP Conference Series: Materials Science and Engineering, IOP Publishing, 012051, 2017

P. Rannou and M. Nechtschein. Aging studies on polyaniline: conductivity and thermal stability. *Synthetic Metals*, 84(1):755–756, 1997.

S. I. A. Razak, A. L. Ahmad, and S. H. S. Zein. Polymerisation of protonic polyaniline/multi-walled carbon nanotubes-manganese dioxide nanocomposites. *J. Phys. Sci*, 20(1):27–34, 2009.

N. Sariciftci, H. Neugebauer, H. Kuzmany, and A. Neckel. In situ ftir spectroscopy of polyaniline. In *Electronic Properties of Conjugated Polymers*, pages 228–231. Springer, 1987.

I. Sedˇ enkovˇ a, M. Trchov´ a, N. V. Blinova, and J. Stejskal. In-situ polymer-´ ized polyaniline films. preparation in solutions of hydrochloric, sulfuric, or phosphoric acid. *Thin Solid Films*, 515(4):1640–1646, 2006.

T. Sharma, S. Aggarwal, S. Kumar, V. Mittal, P. Kalsi, and V. Manchanda. Effect of gamma irradiation on the optical properties of cr-39 polymer. *Journal of materials science*, 42(4):1127–1130, 2007.

H. Shirakawa, E. J. Louis, A. G. MacDiarmid, C. K. Chiang, and A. J. Heeger. Synthesis of electrically conducting organic polymers: halogen derivatives of polyacetylene,(ch) x. *Journal of the Chemical Society, Chemical Communications*, (16):578–580, 1977.

J. P. Sibilia. *A guide to materials characterization and chemical analysis*. John Wiley & Sons, 1996.

Y. Singh. Electrical resistivity measurements: a review. In *International journal of modern physics: Conference series*, volume 22, pages 745–756. World Scientific, 2013.

D. A. Skoog, F. J. Holler, and S. R. Crouch. *Principles of instrumental analysis*. Cengage learning, 2017.

T. A. Skotheim. *Handbook of conducting polymers*. CRC press, 1997.

J. Smith et al. Synthesis of multi-dimensional organic nano-conductors for the enhancement of thermal, electrical, and mechanical properties of composites. 2014.

R. Smith. *Biodegradable polymers for industrial applications*. CRC Press, 2005.

E. Song and J.-W. Choi. Conducting polyaniline nanowire and its applications in chemiresistive sensing. *Nanomaterials*, 3(3):498–523, 2013.

L. Songxi. Electropolymerization 3, 4-study on ethylene dioxythiophene. 2012.

J. Stejskal, J. Prokes, and M. Trchovˇ a. Reprotonation of polyaniline: A route´ to various conducting polymer materials. *Reactive and Functional Polymers*, 68(9):1355–1361, 2008.

A. A. Syed and M. K. Dinesan. Polyaniline—a novel polymeric material. *Talanta*, 38(8):815–837,1991.

P. R. Teasdale, G. M. Spinks, L. A. Kane-Maguire, and G. G. Wallace. *Conductive electroactive polymers: intelligent polymer systems*. CRC press, 2008.

M. Trchova and J. Stejskal. Polyaniline: The infrared spectroscopy of con-´ ducting polymer nanotubes (iupac technical report). *Pure and Applied Chemistry*, 83(10):1803–1817, 2011.

M. Trchova, I.´ Sedˇ enkovˇ a, E. N. Konyushenko, J. Stejskal, P. Holler, and´ G. Ciri´ c-Marjanovi´ c. Evolution of polyaniline nanotubes: the oxidation of´ aniline in water. *The Journal of Physical Chemistry B*, 110(19):9461–9468, 2006.

K. Tzou and R. Gregory. A method to prepare soluble polyaniline salt solutions—in situ doping of pani base with organic dopants in polar solvents. *Synthetic Metals*, 53(3):365–377, 1993.

D. W. Van Krevelen and K. TeNijenhuis. *Properties of polymers: their correlation with chemical structure; their numerical estimation and prediction from additive group contributions*. Elsevier, 2009.

M. Wagner. Synthesis, characterization and chemical sensor application of conducting polymers. 2013.

Y. Wei, X. Tang, Y. Sun, and W. W. Focke. A study of the mechanism of aniline polymerization. *Journal of Polymer Science Part A: Polymer Chemistry*, 27(7):2385–2396, 1989.

Y. Yang and S. Mu.Synthesis and high electrochemical activity of poly(aniline-co-2-amino-4-hydroxybenzenesulfonic acid). *Electrochimica Acta*,54(2):506–512, 2008.

# APPENDICES

## APPENDIX 1

### CALCULATION OF THE THICKNESS OF THIN FILMS

From Table 4.3 the mass, breath and length of the thin films were used in the following calculations. The thickness of the thin film wer calculated using the equation below. Where ;

t = thickness of sample

m = mass of thin film

ρ = density of polyaniline, 1.326 ± 0.014 g/mL

$$t = \frac{m}{\rho A}$$

For PANI-HCl : m = 0.24 g L = 3.10 cm Breath = 1.20 cm

$$t = \frac{0.24}{3.10\ x\ 1.20\ x\ 1.326}$$

$$t = 0.048 \times 10^{-4}\ \mu m$$

For PANI-$H_2SO_4$: m = 0.17 g L = 2.80 cm Breath = 1.20 cm

$$t = \frac{0.17}{2.80\ x\ 1.20\ x\ 1.326}$$

$$t = 0.038 \times 10^{-4}\ \mu m$$

For PANI- $HNO_3$: m = 0.25 g  L = 3.10 cm  Breath = 1.20 cm

$$t = \frac{0.25}{3.10 \ x \ 1.20 \ x \ 1.326}$$

$$t = 0.051 \times 10^{-4} \ \mu m$$



For PANI- $CH_3COOH$: m = 0.15 g  L = 3.00 cm  Breath = 1.20 cm

$$t = \frac{0.15}{3.00 \ x \ 1.20 \ x \ 1.326}$$

$$t = 0.031 \times 10^{-4} \ \mu m$$

NOTE: The thickness of the bulk samples were measured with micrometer screw-guage and presented in the Table 4.4

## APPENDIX 2

## CALCULATIONS OF ELECTRICAL RESISTIVITY AND CONDUCTIVITY OF THIN FILMS

From Table 4.5 the resistivity and conductivity of the thin films are presented. The average voltage and average current were used in the calculations as presented below using the equations below:

$$\rho = 4.5324t\frac{V}{I}$$

and

$$\sigma = \frac{1}{\rho}$$

For PANI-HCl: I = 2.00 mA V = 3.10 mV t = 0.048 x $10^{-4}$ μm

$$\rho = 4.5324 \times 0.048 \times \frac{3.10}{2.00}$$

$$\rho = 0.3372\ \Omega.cm$$

$$\sigma = 2.966\ S.cm^{-1}$$

For PANI- $H_2SO_4$: I = 2.00 mA  V = 3.40 mV  t = 0.038 x $10^{-4}$ μm

$$\rho = 4.5324 \times 0.038 \times \frac{3.40}{2.00}$$

$$\rho = 0.292\ \Omega.cm$$

$$\sigma = 3.424\ S.cm^{-1}$$

For PANI- $HNO_3$: I = 2.00 mA  V = 8.60 mV  t = 0.051 x $10^{-4}$ μm

$$\rho = 4.5324 \times 0.051 \times \frac{8.60}{2.00}$$

$$\rho = 0.994\ \Omega.cm$$

$$\sigma = 1.006\ S.cm^{-1}$$

For PANI- $CH_3COOH$: I = 2.00 mA  V = 14.20 mV  t = 0.031 x $10^{-4}$ μm

$$\rho = 4.5324 \times 0.031 \times \frac{14.20}{2.00}$$

$$\rho = 0.998\ \Omega.cm$$

$$\sigma = 1.002\ S.cm^{-1}$$

## CALCULATIONS OF ELECTRICAL RESISTIVITY AND CONDUCTIVITY OF BULK SAMPLES

For PANI-HCl: I = 1.95 mA V = 2.00 mV t = $0.322 \times 10^{-4}$ µm

$$\rho = 4.5324 \times 0.322 \times \frac{2}{1.95}$$

$$\rho = 1.497\ \Omega.cm$$

$$\sigma = 0.669\ S.cm^{-1}$$

For PANI- $H_2SO_4$: I = 2.35 mA V = 1.00 mV t = $0.438 \times 10^{-4}$ µm

$$\rho = 4.5324 \times 0.438 \times \frac{1}{2.35}$$

$$\rho = 0.845\ \Omega.cm$$

$$\sigma = 1.183\ S.cm^{-1}$$

For PANI- $HNO_3$: I = 0.35 mA V = 0.70 mV t = 0.367 x $10^{-4}$ μm

$$\rho = 4.5324 \times 0.367 \times \frac{0.70}{0.35}$$

$$\rho = 3.326\ \Omega.cm$$

$$\sigma = 0.300\ S.cm^{-1}$$

For PANI- $CH_3COOH$: I = 0.25 mA V = 1.00 mV t = 0.371 x $10^{-4}$ μm

$$\rho = 4.5324 \times 0.367 \times \frac{1.00}{0.25}$$

$$\rho = 6.726\ \Omega.cm$$

$$\sigma = 0.148\ S.cm^{-1}$$